Table 1 The characteristics of patients with fulminant myocarditis using ECMO (F group)

Age, gender	Time interval to application (h)	Inotropic agents before support	Indication for support	Haemodynamics					Echocardiography				IABP	Pacing	Outcomes
				SBP (mmHg)	HR (b.p.m)	RA (mmHg)	PCW (mmHg)	CI (L/min/m^2)	MR	TR	IVCd (mm)	Pericardial effusion			
67 years, F	20	DA16, DB8, NE0.2, E0.14	Hypotension	80	111	12	24	1.4	−	−	18	+	Y	N	Dead
59 years, M	18	DA6, DB10	Hypotension	94	136	10	16	3.1	−	−	21	+	Y	N	Weaned
22 years, F	12	DA5, DB10	VT/VF	86	120	12	18	1.9	+	−	14	+	Y	N	Weaned
37 years, M	36	DA11, DB6, NE0.3	Hypotension	64	152	17	29	2.7	+	−	29	+	Y	N	Weaned
32 years, F	26	DA3, DB3	VT/VF	76	126	13	16	2.1	+	+	21	+	N	Y	Weaned
53 years, F	26	DA20, DB20	Cardiac arrest	NM	NP						15	+	N	N	Dead
24 years, M	7	DB3	Hypotension	84	122	10	25	1.4	+	−	20	+	N	N	Weaned
29 years, M	14	DA5	VT/VF	60	180	20	25	4.3	−	−	18	+	N	Y	Weaned
16 years, M	11	DA11	Hypotension	80	117	17	21	2.0	−	−	19	+	Y	N	Dead
54 years, F	8	DA3, DB3	VT/VF	90	156	17	28	2.9	+	−	22	+	N	Y	Weaned
49 years, F	15	DB3	Hypotension	60	110	16	19	1.7	+	−	15	+	N	N	Weaned
22 years, F	18	DA27, DB27	Hypotension	53	150	15	25	1.9	−	−	19	+	N	N	Weaned
31 years, M	12	DA10, DB15, NE0.5	Hypotension	88	132	2	21	2.2	++	+	19	+	N	N	Weaned
42 years, M	15	DA5	Hypotension	47	70[a]	15	30	1.4	+	−	17	+	Y	Y	Dead

SBP, systolic blood pressure; HR, heart rate; RA, right atrial pressure; PCW, pulmonary capillary wedge pressure; CI, cardiac index; MR, mitral valve regurgitation; TR, tricuspid valve regurgitation; IVCd, inferior vena cava dimension size; DA, dopamine; DB, dobutamine; NE, norepinephrine; E, epinephrine; VT/VF means the existence of ventricular tachycardia or ventricular fibrillation; NM, not measured; NP, not palpable.

[a]Heart rate by temporary right ventricular pacing.

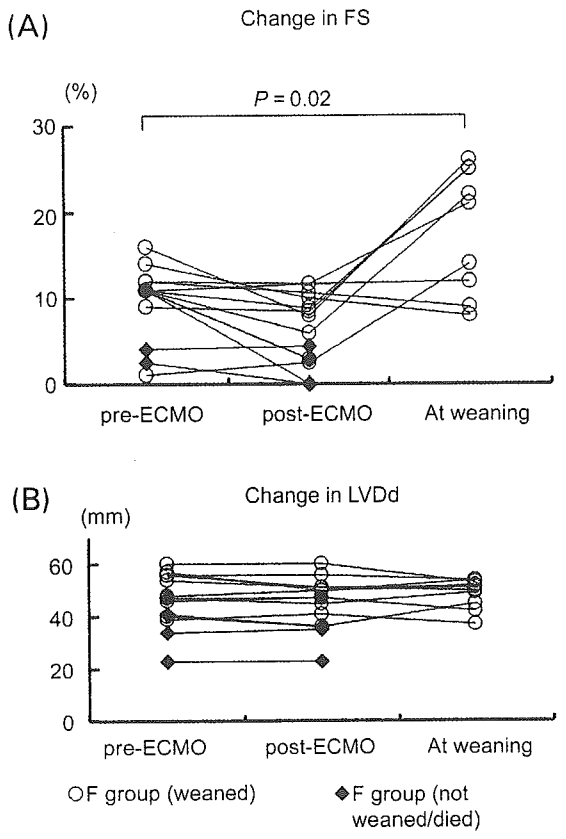

Figure 2 Acute changes in left ventricular function before and immediately after the support and at weaning from ECMO in patients with fulminant myocarditis (F group). (*A*) FS and (*B*) LVDd. Open circles indicate patients who were weaned from ECMO and closed diamonds indicate F patients who were not weaned from ECMO and died.

Discussion

This study demonstrated that ~70% of patients with fulminant myocarditis supported by percutaneous ECMO could be saved. Cardiac function was severely depressed in the acute phase but improved markedly in the chronic phase. The clinical course in the chronic phase in the patients with fulminant myocarditis who were weaned from ECMO was similar to that in patients with non-fulminant myocarditis.

Survival and percutaneous ECMO

McCarthy *et al.*[8] reported that fulminant myocarditis is a distinct clinical entity with an excellent long-term prognosis. However, there were few patients requiring circulatory supports in their reports, and the clinical outcome of those patients remains undetermined. In our series of patients, even though cardiac function was severely depressed in the acute phase reaching zero myocardial FS, haemodynamic volume support by percutaneous ECMO could effectively prevent the development of multiple organ failure. When compared with left ventricular assist devices, which we used to treat 106 patients with deteriorated haemodynamics since 1982, percutaneous ECMO has an advantage in terms of its quick, easy, and less invasive application,[4-6] which may help in overcoming potential complications such as stroke, peripheral arterial ischaemia, haemorrhage, and infections.[16] If there is no improvement in cardiac function, the patients should be bridged from ECMO to ventricular assist devices. The present study includes only one bridged patient. The results derived from other studies of fulminant myocarditis showed a survival rate of 40–50% for patients supported with ventricular assist devices.

Patients with fulminant myocarditis may be better managed by maintaining circulatory support than pursuing transplantation. As reported previously, the survival rate of patients with post-cardiotomy shock who required ECMO but had already suffered from irreversible myocardial damage was 20–40%.[17] However, the present study demonstrated that many of these patients (≈70%) have a reasonable chance for full cardiac recovery and benefit from several days or weeks of circulatory support using ECMO, without undergoing transplantation. Particularly for children in whom transplantation is certainly not encouraging, ECMO is useful in delaying transplantation by providing support sufficiently long to determine whether cardiac function may improve.[18]

Temporary myocardial damage in patients with fulminant myocarditis

In the present study of fulminant myocarditis, patients who were not weaned from ECMO and died exhibited a higher peak CK-MB level and a more depressed systolic function (lower FS) than those who were weaned from ECMO. Interestingly, despite similar peak CK-MB levels, there was a significant difference in FS between patients with fulminant myocarditis who were weaned from ECMO and those with non-fulminant myocarditis. These findings indicate that the extent of myocardial dysfunction and necrosis caused by inflammatory responses may determine the acute outcome in myocarditis patients. Moreover, it is speculated that the echocardiographic finding of less dilatation may be related to a severe infectious insult with myocardial oedema. In light of accumulating evidence, myocardial dysfunction is associated with cardiodepressant mediators including free radicals and inflammatory cytokines.[19,20] From the current data shown in *Figure 2*, percutaneous ECMO does not appear to directly promote functional recovery. However, it may be useful in supporting a compromised heart until the inflammatory storm in the myocardium has subsided. Potential therapies specific for the pathophysiological process of acute myocarditis include immunomodulation (i.e. immunoglobulin and interferon)[21-23] and vaccination,[24,25] the use of which may provide new insights into the treatment of this disease. Duncan *et al.*[7] reported that mechanical circulatory support in combination with immunotherapy (intravenous administration of gamma globulin and/or steroids) results in 60% of the acute survival of children with fulminant myocarditis.

Recovery of ventricular function and long-term outcome

In patients with fulminant myocarditis who survived, FS improved in the chronic phase to a level similar to that in patients with acute non-fulminant myocarditis. The present results were different from those reported previously by Felker *et al.*[26] They reported a significant improvement in FS in patients with fulminant myocarditis (from 19±4 to 30 ± 8%), whereas no improvement was

Table 2 Comparison between patients who were weaned and those who were not weaned from ECMO in the F group

	Patients who were weaned ($n = 10$)	Patients who were not weaned/died ($n = 4$)	*P*-value
Aspartate aminotransferase (IU/L)	145 (108–381)	280 (208–3775)	0.138
Alanine aminotransferase (IU/L)	70 (54–358)	81 (60–2123)	0.524
Lactate dehydrogenase (IU/L)	635 (475–1229)	1222 (630–6301)	0.358
Peak CPK (IU/L)	3860 (1097–6168)	12005 (7167–16117)	0.138
Peak CK-MB (IU/L)	102 (16–134)	229 (200–538)	0.042
Blood urine nitrogen (mg/dL)	18.5 (15–26)	34.5 (30–38.5)	0.004
Serum creatinine (mg/dL)	1.0 (0.8–1.1)	2.4 (1.55–2.6)	0.179
White blood cell count (/μL)	11635 (9230–12200)	8535 (6400–12885)	0.289
C-reactive protein (mg/dL)	10.2 (6.6–12.4)	7.9 (4.5–15.1)	0.832

The median (25–75%) data. All data except peak creatine phosphokinase (CPK) and its isoform (CK-MB) are presented as baseline (measured on admission).

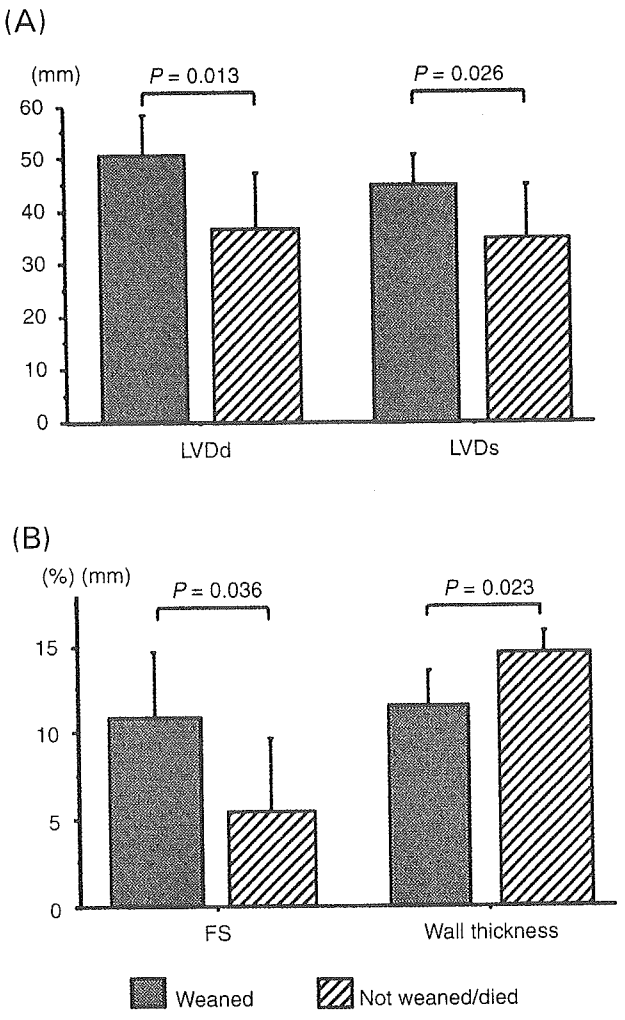

Figure 3 Comparison of echocardiographic data between patients who were weaned and those who were not weaned from ECMO in F group. All these data were gathered on admission. (*A*) LVDd and LVDs. (*B*) FS and ventricular wall thickness.

observed in those with acute myocarditis (from 17±7 to 19 ± 7%). We also noted that the percentages of adverse clinical events were similar between the two groups during the follow-up period. Only one patient in the present study group was rehospitalized due to heart failure. However, the previous studies showed that the long-term outcome of patients with acute myocarditis was poor, that is, 50–60% of patients had a 5-year survival rate, compared with those with fulminant myocarditis.[8,27,28] This difference may be due to the differences in patients' clinical backgrounds. In the present study, all the 14 patients with fulminant myocarditis and 12 of 13 patients with non-fulminant acute myocarditis had a distinct onset of cardiac symptoms within a short duration from flu-like symptoms and had no recurrence of myocarditis. The myocarditis cases observed in the present study appear to be more acute than those reported by others.[8,28] In the previous studies, designed on the basis of the classification of Lieberman's report,[29] enrolled patients with acute non-fulminant myocarditis had heart failure without a distinct onset of cardiac symptoms, which lasted for a period of weeks to months. The timing of cardiac symptom presentation may be associated with the pathophysiology and/or the state of myocarditis. Patients in the previous studies may have included those with acute myocarditis without distinct onset and/or chronic (active or persistent) myocarditis. Kodama *et al.*[30] showed the long-term favourable outcome of acute myocarditis patients with a distinct onset classified by clinical subtypes, compared with those without a distinct onset. Patients with myocarditis without a distinct onset may have already undergone the remodelling process following a viral infection, leading to dilated cardiomyopathy. Thus, the clinical presentation may play an important role in the prognosis of this particular disease.[31]

Study limitations

This study has a few potential limitations. First, this is a retrospective cohort study performed at one centre. The number of patients was too small to permit multivariate analysis with adjustment for underlying confounders. However, the clinical relevance of the findings regarding such a rare but life threatening disease allows the present comparison. Secondly, endomyocardial biopsy was not performed in all the patients. Endomyocardial biopsy is of value in evaluating the activity of inflammation and identifying infiltrating cells. However, Dec *et al.*[32] demonstrated that the combination of the clinical features of viral myocarditis and subsequent substantial improvement in the left ventricular function suggest the clinical diagnosis of active myocarditis, even when supportive biopsy evidence

Table 3 Comparison with laboratory data between F groups and NF (non-fulminant acute myocarditis) groups

	F group ($n = 14$)	NF group ($n = 13$)	P-value
Aspartate aminotransferase (IU/L)	188 (108-381)	46 (39-127)	0.006
Alanine aminotransferase (IU/L)	70 (57-358)	42 (27-69)	0.051
Lactate dehydrogenase (IU/L)	711 (477-1229)	361 (175-491)	0.004
Peak CPK (IU/L)	3903 (1765-11667)	529 (253-1042)	<0.001
Peak CK-MB (IU/L)	117 (67-210)	98 (67-124)	0.447
Blood urine nitrogen (mg/dL)	24 (16-32)	11 (9-19)	0.003
Serum creatinine (mg/dL)	1.0 (0.8-1.6)	0.75 (0.6-0.85)	0.004
White blood cell count (/μL)	11385 (9049-12200)	9030 (7550-9918)	0.099
C-reactive protein (mg/dL	9.9 (5.4-12.4)	3.6 (2.6-12.3)	0.201

The median (25-75%) data. All data except peak creatine phosphokinase (CK) and its isoform (CK-MB) are presented as baseline (measured on admission).

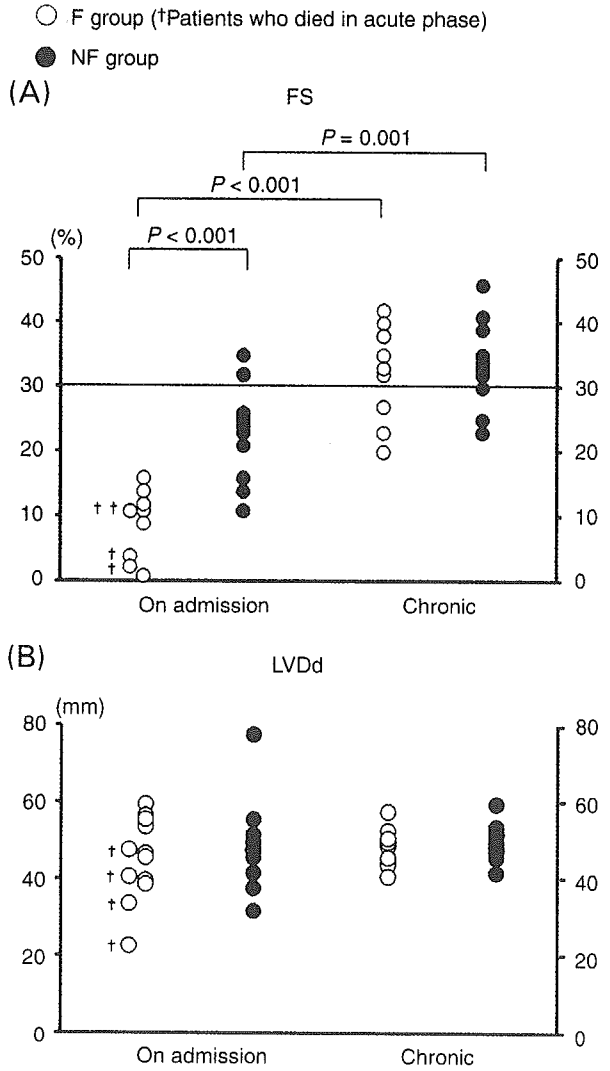

Figure 4 Changes in FS (*A*) and LVDd (*B*) (determined by echocardiography) on admission, in the chronic phase (~6-12 months after). Open circles indicate F group, closed circles indicate non-fulminant acute myocarditis (NF) group, and crosses indicate patients who died.

is lacking. In the present study, as shown in *Figure 4*, left ventricular function recovered to almost normal in the chronic phase and was not accompanied by cardiac dilatation or remodelling. Thus, biopsy was deemed unnecessary;

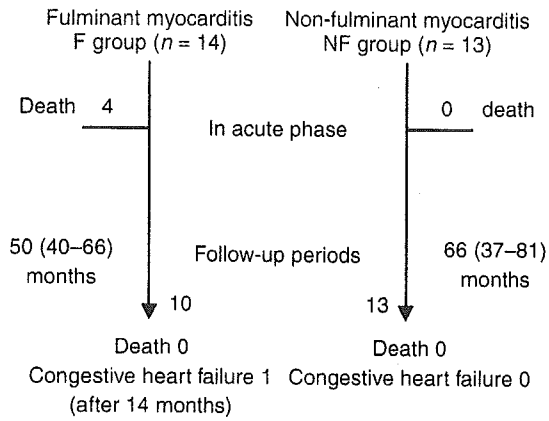

Figure 5 Clinical events in follow-up period.

in some cases, it is difficult to obtain informed consent from the patients of this study.

In conclusion, percutaneous ECMO is a highly effective form of haemodynamic support for patients with fulminant myocarditis. Once a patient recovers from inflammatory myocardial damage, the subsequent clinical outcome is favourable, similar to that observed in patients with acute non-fulminant myocarditis. A further study is required to determine the potential trigger promoting the remodelling process following viral myocarditis.

References

1. Cooper LT Jr. *Myocarditis: from Bench to Bedside*. Totowa, New Jersey: Humana Press; 2003.
2. Liu P, Mason J. Advances in the understanding of myocarditis. *Circulation* 2001;104:1076-1082.
3. Feldmann AM, McNamara D. Myocarditis. *N Eng J Med* 2000;343: 1388-1398.
4. Kato S, Morimoto S, Hiramatsu S, Nomura M, Ito T, Hishida H. Use of percutaneous cardiopulmonary support of patients with fulminant myocarditis and cardiogenic shock for improving prognosis. *Am J Cardiol* 1999;83:623-625.
5. Chen JM, Spanier TB, Gonzalez JJ, Marelli D, Flannery MA, Tector KA, Cullinane S, Oz MC. Improved survival using external pulsatile mechanical ventricular assistance. *J Heart Lung Transplant* 1999;18:351-357.
6. Acker MA. Mechanical circulatory support for patients with acute-fulminant myocarditis. *Ann Thorac Surg* 2001;71:S73-S76.
7. Duncan BW, Bohn DJ, Atz AM, French JW, Laussen PC, Wessel DL. Mechanical circulatory support for treatment of children with acute fulminant myocarditis. *J Thorac Cardiovasc Surg* 2001;122:440-448.

8. McCarthy RE III, Boehmer JP, Hruban RH, Hutchins GM, Kasper EK, Hare JM, Baughman KL. Long-term outcome of fulminant myocarditis as compared with acute (nonfulminant) myocarditis. *N Eng J Med* 2000;**342**:690-695.
9. Swan HJC, Forrester JS, Diamond G, Chatterjee K, Parmley WW. Hemodynamic spectrum of myocardial infarction and cardiogenic shock. *Circulation* 1972;**45**:1097-1110.
10. Sasako Y, Nakatani T, Nonogi H, Miyazaki S, Kito Y, Takano H, Kawashima Y. Clinical experience of percutaneous cardiopulmonary support. *Artif Organs* 1996;**20**:733-736.
11. Schiller NB, Shah PM, Crawford M, DeMaria A, Devereux R, Feigenbaum H, Gutgesell H, Reichek N, Sahn D, Schnittger I, Silverman NH, Tajik AJ. Recommendation for quantification of the left ventricle by two-dimensional echocardiography. American Society of Echocardiography Committee on Standards, Subcommittee on Quantitation of Two-Dimensional Echocardiograms. *J Am Soc Echocardiogr* 1989;**2**:358-367.
12. Kircher BJ, Himelman RB, Shiller NB. Non invasive estimation of right atrial pressure from the respiratory collapse of the inferior vena cava. *Am J Cardiol* 1999;**66**:493-496.
13. Nakatani T, Takano H, Beppu S, Noda H, Taenaka Y, Kumon K, Kito Y, Fujita T, Kawashima Y. Practical assessment of natural heart function using echocardiography in mechanically assisted patients. *ASAIO Trans* 1991;**37**: M420-M421.
14. Aretz HT. Myocarditis: the Dallas criteria. *Hum Pathol* 1987;**18**:619-624.
15. Takano H, Nakatani T. Ventricular assist systems: experience in Japan with Toyobo pump and Zeon pump. *Ann Thorac Surg* 1996;**61**: 317-322.
16. Pagani FD, Aaronson KD, Swaniker F, Bartlett RH. The use of extracorporeal life support in adult patients with primary cardiac failure as a bridge to implantable left ventricular assist device. *Ann Thorac Surg* 2001;**71**: S77-S81.
17. Magovern GJ, Kathleen A, Simpson KA. Extracorporeal membrane oxygenation for adult cardiac support: the Allegheny experience. *Ann Thorac Surg* 1999;**68**:655-661.
18. Pennington DG, Smedira NG, Samuels LE, Acker MA, Curtis JJ, Pagani FD. Mechanical circulatory support for acute heart failure. *Ann Thorac Surg* 2001;**71**(Suppl. 3):S56-S59.
19. Sasayama S, Matsumori A, Kihara Y. New insights into the pathophysiological role for cytokines in heart failure. *Cardiovasc Res* 1999;**42**: 557-564.
20. Mann DL. Inflammatory mediator and failing heart: past, present and foreseeable future. *Circ Res* 2002;**91**:988-998.
21. Drucker NA, Colan SD, Lewis AB, Beiser AS, Wessel DL, Takahashi M, Baker AL, Perez-Atayde AR, Newburger JW. Gamma-globulin treatment of acute myocarditis in the pediatric population. *Circulation* 1994;**89**:252-257.
22. McNamara DM, Rosenblum WD, Janosko KM, Trost MK, Villaneuva FS, Demetris AJ, Murali S, Feldman AM. Intravenous immune globulin in the therapy of myocarditis and acute cardiomyopathy. *Circulation* 1997;**95**: 2476-2478.
23. Kuhl U, Pauschinger M, Schwimmbeck PL, Seeberg B, Lober C, Noutsias M, Poller W, Schultheiss HP. Interferon-beta treatment eliminates cardiotropic viruses and improvement left ventricular function in patients with myocardial persistence of viral genomes and left ventricular dysfunction. *Circulation* 2003;**107**:2793-2798.
24. Kishimoto C, Takada H, Hiraoka Y, Shinohara H, Kitazawa M. Protection against murine Coxackievirus B3 myocarditis by T cell vaccination. *J Mol Cell Cardiol* 2000;**32**:2269-2277.
25. Matsumoto Y, Jee Y, Sugisaki M. Successful TCR-based immunotherapy for autoimmune myocarditis with DNA vaccines after rapid identification of pathogenic TCR. *J Immunol* 2000;**164**:2248-2254.
26. Felker GM, Boehmer JP, Hruban RH, Hutchins GM, Kasper EK, Baughman KL, Hare JM. Echocardiographic findings in fulminant and acute myocarditis. *J Am Coll Cardiol* 2000;**36**:227-232.
27. Mason JW, O'Connell JB, Herskowitz A, Rose NR, McManus BM, Billingham ME, Moon TE. A clinical trial of immunosuppressive therapy for myocarditis. The Myocarditis Treatment Trial Investigators. *N Eng J Med* 1995; **333**:269-275.
28. Grogan M, Redfield MM, Bailey KR, Reeder GS, Gersh BJ, Edwards WD, Rodeheffer RJ. Long-term outcome of patients with biopsy-proved myocarditis: comparison with idiopathic dilated cardiomyopathy. *J Am Coll Cardiol* 1995;**26**:80-84.
29. Lieberman EB, Hutchins GM, Herskowitz A, Rose NR, Baughman KL. Clinicopathologic description of myocarditis. *J Am Coll Cardiol* 1991; **18**:1617-1626.
30. Kodama M, Oda H, Okabe M, Aizawa Y, Izumi T. Early and long-term mortality of the clinical subtypes of myocarditis. *Jpn Circ J* 2001;**65**: 961-964.
31. D'Ambrosio A, Patti G, Manzoli A, Sinagra G, Di Lenarda A, Silvestri F, Di Sciascio G. The fate of acute myocarditis between spontaneous improvement and evolution to dilated cardiomyopathy: a review. *Heart* 2001;**85**:499-504.
32. Dec GW Jr, Palacios IF, Fallon JT, Aretz HT, Mills J, Lee DC, Johnson RA. Active myocarditis in the spectrum of acute dilated cardiomyopathies. Clinical features, histologic correlates, and clinical outcome. *N Eng J Med* 1985;**312**:885-890.

An Association Between Proteinuria and Coronary Atherosclerosis in Patients With Abnormal Glucose Tolerance

Yu-Kataoka, Satoshi Yasuda, Masaysohi Takeno, Shinzo Miyamoto, Isao Morii, Atsushi Kawamura, Shunichi Miyazaki, National Cardiovascular Center, Osaka, Japan

Background: Altered renal function (decrease in creatinine clearance or proteinuria) is an independent risk factor of cardiovascular morbidity and mortality. The present study investigated whether a significant association exists between proteinuria and the extent of coronary atherosclerosis in patients with angina pectoris.

Methods: A total of 490 patients were studied and divided into the following three groups according to the urinary protein (UP) level; normal (UP < 30mg/dl, n=381), low (30<= UP = 100mg/dl, n=66) and high (UP >= 100mg/dl, n=43). Metabolic profiles including hemoglobin (Hb) A1c, fasting glucose and postprandial glucose levels were measured. All major coronary trees were assessed by computer-assisted quantitative coronary angiography. We defined segments with an absolute diameter of <= 1.5mm as diseased lesions and determined average lesion length (ALL).

Results: Patients in the high UP group showed longer ALL and higher levels of HbA1c, fasting and postprandial glucose than other two groups. By multivariate analysis, the UP and postprandial glucose levels were independent determinant of long coronary artery lesions (ALL > 10mm).

Conclusion: These findings indicate that proteinuria is strongly associated with diffuse coronary narrowing. Postprandial hyperglycemia may contribute to a preferential link between atherosclerotic macrovascular disease and renal microvascular disease.

Table:

	fasting blood glucose (mg/dl)	postprandial blood glucose (mg/dl)	HbA1c (%)	ALL (mm)
normal UP (< 30 mg/dl)	106 ± 26	184 ± 69	6.0 ± 1.1	10.7 ± 8.1
low UP (30 ≤ UP < 100 mg/dl)	106 ± 27	184 ± 69	6.3 ± 1.2	10.6 ± 6.1
high UP (≥ 100 mg/dl)	129 ± 46☆#	221 ± 69☆#	7.0 ± 1.3☆#	14.2 ± 8.8☆#

☆ p<0.05 vs normal UP, # p<0.05 vs low UP (by analysis of variance)

THE JOURNAL OF BIOLOGICAL CHEMISTRY VOL. 281, NO. 11, pp. 7205–7213, March 17, 2006

Functions of the Cytoplasmic Tails of the Human Receptor Activity-modifying Protein Components of Calcitonin Gene-related Peptide and Adrenomedullin Receptors*[S]

Received for publication, October 13, 2005, and in revised form, January 6, 2006 Published, JBC Papers in Press, January 11, 2006, DOI 10.1074/jbc.M511147200

Kenji Kuwasako[‡1], Yuan-Ning Cao[‡], Chun-Ping Chu[§], Shuji Iwatsubo[‡], Tanenao Eto[‡], and Kazuo Kitamura[‡]

From the [‡]First and [§]Third Departments of Internal Medicine, Miyazaki Medical College, University of Miyazaki, Miyazaki 889-1692, Japan

Receptor activity-modifying proteins (RAMPs) enable calcitonin receptor-like receptor (CRLR) to function as a calcitonin gene-related peptide receptor (CRLR/RAMP1) or an adrenomedullin (AM) receptor (CRLR/RAMP2 or -3). Here we investigated the functions of the cytoplasmic C-terminal tails (C-tails) of human RAMP1, -2, and -3 (hRAMP1, -2, and -3) by cotransfecting their C-terminal deletion or progressive truncation mutants into HEK-293 cells stably expressing hCRLR. Deletion of the C-tail from hRAMP1 had little effect on the surface expression, function, or intracellular trafficking of the mutant heterodimers. By contrast, deletion of the C-tail from hRAMP2 disrupted transport of hCRLR to the cell surface, resulting in significant reductions in ^{125}I-hAM binding and evoked cAMP accumulation. The transfection efficiency for the hRAMP2 mutant was comparable with that for wild-type hRAMP2; moreover, immunocytochemical analysis showed that the mutant hRAMP2 remained within the endoplasmic reticulum. FACS analysis revealed that deleting the C-tail from hRAMP3 markedly enhances AM-evoked internalization of the mutant heterodimers, although there was no change in agonist affinity. Truncating the C-tails by removing the six C-terminal amino acids of hRAMP2 and -3 or exchanging their C-tails with one another had no effect on surface expression, agonist affinity, or internalization of hCRLR, which suggests that the highly conserved Ser-Lys sequence within hRAMP C-tails is involved in cellular trafficking of the two AM receptors. Notably, deleting the respective C-tails from hRAMPs had no effect on lysosomal sorting of hCRLR. Thus, the respective C-tails of hRAMP2 and -3 differentially affect hCRLR surface delivery and internalization.

CGRP[2] and AM belong to the calcitonin family of regulatory molecules and exert a wide variety of biological effects, including potent vasorelaxation (1–3). The receptors that mediate these effects are heterodimers composed of CRLR and RAMP, a novel accessory protein (4). The three RAMP isoforms (RAMP1, RAMP2, and RAMP3) are each composed of ~160 amino acids, and all exhibit a common structure that includes a large extracellular N-terminal domain, a single membrane-spanning domain, and a very short C-tail, but they share less than 30% sequence identity and differ in their tissue distributions (4, 5). When acting as a chaperone, each RAMP forms a 1:1 heterodimer with CRLR, probably in the ER (4, 6). They then mediate the transport of CRLR to the cell surface, where the heterodimers form functional CGRP or AM receptors: CRLR/RAMP1 forms the $CGRP_1$ receptor (4), which can also be activated by high concentrations of AM (7, 8); CRLR/RAMP2 forms an AM-specific receptor that is sensitive to the AM receptor antagonist AM-(22–52) (AM_1 receptor) (7, 9); and CRLR/RAMP3 forms an AM receptor that is sensitive to both the $CGRP_1$ receptor antagonist CGRP-(8–37) and AM-(22–52) (AM_2 receptor) (7, 9). It is the RAMP extracellular domain that mediates agonist binding to CRLR/RAMP heterodimers (11–13), which in turn mediate intracellular cAMP production and Ca^{2+} mobilization (4, 10).

Exposing cells that express GPCRs to their respective agonists frequently leads to a rapid internalization of the receptor in a process believed to involve clathrin-coated vesicles, caveolin-rich vesicles, or both (14, 15). The internalized GPCRs may be recycled back to the plasma membrane in order to promote functional restoration of signal transduction, or they may be trafficked to lysosomes, where they are degraded (14, 15). Similarly, upon binding their respective agonist, hCRLR/RAMP heterodimers stably expressed in HEK-293 cells are rapidly internalized without dissociation via clathrin-coated vesicles (6, 10) in a process that is blocked by dominant negative mutants of dynamin and β-arrestin 2 (6). In that regard, it is well known that G protein-coupled receptor kinases phosphorylate serine/threonine sites located in many GPCR C-tails, enabling β-arrestins to bind there (16). After internalization, both CRLR and RAMP are targeted to lysosomes (10), where they are degraded (6).

Although short, the RAMP C-tails do contain potential sites of interaction with other proteins (5, 17). For instance, the hRAMP3 C-tail possesses a classical type I PDZ (PSD-95/Disc-large/ZO-1) binding motif (TLL) (5, 17), and the binding of NSF to the PDZ motif of hRAMP3 was found to promote slow recycling of internalized hCRLR/hRAMP3 heterodimers in HEK-293 cells (18). In addition, a five-residue motif (QSKRT) in the hRAMP1 C-tail can act as an ER retention signal (19). The C-tails of RAMPs, like that of CRLR, also contain potential phosphorylation and ubiquitination sites (5, 17). Ubiquitination is the post-translational attachment of ubiquitin lysine residues in the substrate proteins (20, 21); it is not crucial for receptor internalization but is essential for proper trafficking to lysosomes for degradation (22, 23). Whether the phosphorylation and ubiquitination sites are also involved

* This work was supported in part by grants-in-aid for scientific research on priority areas and for the 21st Century Centers of Excellence Program (Life Science) from the Ministry of Education, Culture, Sports, Science, and Technology, Japan. The costs of publication of this article were defrayed in part by the payment of page charges. This article must therefore be hereby marked "*advertisement*" in accordance with 18 U.S.C. Section 1734 solely to indicate this fact.

[S] The on-line version of this article (available at http://www.jbc.org) contains one supplemental figure.

[1] To whom correspondence should be addressed. Tel.: 81-985-85-0872; Fax: 81-985-85-6596; E-mail: kuwasako@fc.miyazaki-med.ac.jp.

[2] The abbreviations used are: CGRP, calcitonin gene-related peptide; hαCGRP, human αCGRP; AM, adrenomedullin; hAM, human AM; CRLR, calcitonin receptor-like receptor; hCRLR, human CRLR; RAMP, receptor activity-modifying protein; C-tail, cytoplasmic C-terminal tail; ER, endoplasmic reticulum; GPCRs, G protein-coupled receptors; NSF, *N*-ethylmaleimide-sensitive factor; hNSF, human NSF; PDZ, PSD-95/Disc-large/ZO-1; FITC, fluorescein isothionate; PE, phycoerythrin; HEK, human embryonic kidney; GFP, green fluorescent protein; FACS, fluorescence-activated cell sorting; PBS, phosphate-buffered saline; NHERF, Na^+/H^+ exchanger regulatory factor; β_2-AR, β_2-adrenergic receptor.

in intracellular trafficking of CRLR/RAMP heterodimers remains unknown. To address that issue, we examined the effects of expressing various hRAMP C-tail deletion and progressive truncation mutants and chimeras in which the C-tails were exchanged among the three hRAMPs in HEK-293 cells stably expressing hCRLR.

EXPERIMENTAL PROCEDURES

Materials—^{125}I-[Tyr^0]hαCGRP (specific activity 2 μCi/pmol) (24), which contains an extra N-terminal tyrosine residue (Tyr^0), and ^{125}I-hAM (specific activity 2 μCi/pmol) (1) were both produced in our laboratory. Human αCGRP was purchased from Peptide Institute (Osaka, Japan). [Tyr^0]hαCGRP was from Phoenix Pharmaceuticals, Inc. Human AM was kindly donated by Shionogi & Co. (Osaka, Japan). Mouse anti-hNSF antibody was from Calbiochem. Mouse anti-V5 antibody and FITC-conjugated mouse anti-V5 monoclonal antibody (anti-V5-FITC antibody) were from Invitrogen. Rabbit anti-calnexin antibody was from Stressgen Biotechnologies Corp. (Victoria, Canada), and Alexa Fluor® 594 (biotin- and fluorescent dye-labeled goat anti-rabbit IgG antibody) were from Molecular Probes, Inc. (Eugene, OR). PE-conjugated rabbit anti-mouse secondary antibody was from Exalpha Biologicals, Inc. All other reagents were of analytical grade and were obtained from various commercial suppliers.

Expression Constructs—hNSF (GenBank™ accession number BC030613) was cloned from cDNA obtained from human heart (Clontech) using PCR with the appropriate primers and then modified to provide a consensus Kozak sequence as previously described (25). hRAMP1, -2, and -3 (4) were also modified to provide the same Kozak sequence. A double V5 epitope tag (GKPIPNPLLGLDST) was ligated, in frame, to the 5′-end of the cDNAs encoding each intact hRAMP, and the native signal sequences were removed and replaced with MKTILALSTYIFCLVFA (26), yielding V5-hRAMP1, -2, and -3. The deletion and progressive truncation mutations in the V5-hRAMP C-tails were created by using 3′-primers that introduced a translational stop codon at the desired positions (Fig. 1); with RAMP3, for instance, Δ139 represents a mutant in which a stop codon was introduced after residue 139. In addition, various V5-hRAMP chimeras were constructed by exchanging the 9 C-terminal amino acid residues among the three hRAMPs. The hNSF, V5-hRAMPs, V5-hRAMP deletion and truncation mutants, and V5-hRAMP chimeras were then respectively cloned into the mammalian expression vector pCAGGS/Neo (10) using the 5′-XhoI and 3′-NotI sites, and the sequences of the resultant constructs were all verified using an Applied Biosystems 310 Genetic Analyzer. The individual V5-hRAMPs were compared with the native sequence in the assays and were found to behave identically (data not shown).

Cell Culture and DNA Transfection—HEK-293 cells stably expressing a hCRLR-GFP chimera (10) were maintained in Dulbecco's modified Eagle's medium supplemented with 10% fetal bovine serum, 100 units/ml penicillin G, 100 μg/ml streptomycin, 0.25 μg/ml amphotericin B, and 0.25 mg/ml G 418 at 37 °C under a humidified atmosphere of 95% air, 5% CO_2. For experimentation, cells were seeded into 6- or 24-well plates and, upon reaching 70 – 80% confluence, were transiently cotransfected with the indicated cDNAs using Lipofectamine transfection reagents (Invitrogen) according to the manufacturer's instructions. Briefly, the cells were incubated for 4 h in Opti-MEM I medium containing plasmid DNAs, Plus reagent, and Lipofectamine (see Ref. 27 for 6-well and Ref. 11 for 24-well plates). As a control, some cells were transfected with empty vector (mock). All experiments were carried out 48 h after transfection.

FACS Analysis—Flow cytometry was carried out to assess the levels of cell surface expression of V5-hRAMPs, V5-hRAMP truncation

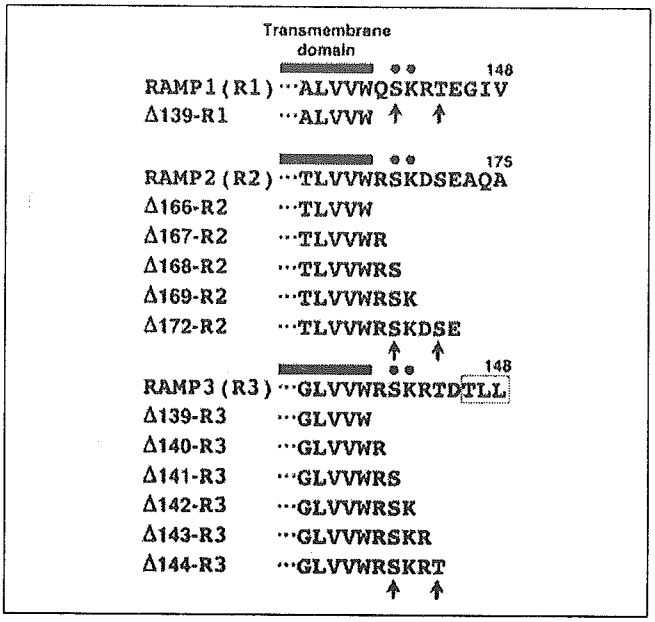

FIGURE 1. **Amino acid sequence alignment of the cytoplasmic tails of hRAMP1, -2, and -3.** The sequences are aligned for maximum homology; alignment of the entire sequences was presented by MacLatchie *et al.* (4). The *numbers* indicate the amino acid positions in accordance with Sexton *et al.* (5). *Black circles* indicate conserved amino acids; *arrows* indicate potential phosphorylation sites; and the PDZ binding motif is *boxed*. The progressive hRAMP C-tail truncation mutants were created using 3′-primers that introduced a translational stop codon at the indicated positions; for instance, Δ139 represents a truncation mutant that introduced a stop codon after residue 139.

mutants, or V5-hRAMP chimeras in HEK-293 cells. To evaluate cell surface expression, cells were harvested following transient transfection, washed twice with PBS, resuspended in ice-cold FACS buffer (27), and then incubated for 60 min at 4 °C in the dark with anti-V5 monoclonal antibody (1:1000 dilution). Following two additional washes with FACS buffer, the cells were incubated for 60 min at 4 °C in the dark with PE-conjugated rabbit anti-mouse secondary antibody (1:400 dilution) in ice-cold FACS buffer. For evaluation of whole cell expression, cells were first permeabilized using IntraPrep™ reagents (Beckman Coulter, Fullerton, CA) according to the manufacturer's instructions and then incubated with anti-V5-FITC antibody (1:500 dilution) for 15 min at room temperature in the dark. Following two successive washes with FACS buffer, both groups of cells were subjected to flow cytometry in an EPICS XL flow cytometer (Beckman Coulter) and analyzed using EXPO 2 software (Beckman Coulter). Fluorophores were excited at 488 nm, and the emission was monitored at 530 nm for GFP and 575 nm for PE. Viability was assessed by exclusion of propidium iodide.

Immunofluorescence Microscopy—HEK-293 cells stably expressing hCRLR-GFP were plated onto 35-mm glass-bottomed dishes (Iwaki, Tokyo, Japan). As determined by the experimental protocol, some cells were then transiently transfected with V5-hRAMP2, Δ166-hRAMP2, or Δ167-hRAMP2. The cells were then fixed with 3.7% formaldehyde in PBS for 20 min at room temperature, washed twice with PBS, and permeabilized with 0.25% Triton X-100 in PBS for 10 min. Thereafter, the cells were incubated at room temperature for 30 min in blocking buffer (PBS containing 1% bovine serum albumin), followed by incubation for 60 min first with rabbit anti-calnexin (1:200 dilution) and mouse anti-V5-FITC antibody (1:500 dilution) and then, after washing four times with PBS, with the Alexa Fluor® 594 diluted 1:100 in blocking buffer. After another three washes with PBS, the cells were mounted using Slow-Fade mounting medium (Molecular Probes, Inc.), and a 22-mm glass coverslip was seated in the center of each dish. Double labeling was

viewed using a TCS-SP2 AOBS confocal laser-scanning microscope (Leica) equipped with a × 63/1.32 numerical aperture immersion lens (Leica).

Whole-cell Radioligand Binding Assays—Transfected HEK-293 cells in 24-well plates were washed twice with prewarmed PBS and then incubated for 5 h at 4 °C with ^{125}I-[Tyr^0]hαCGRP (100 pM) or ^{125}I-hAM (20 pM) in the presence (for nonspecific binding) or absence (for total binding) of 1 μM unlabeled hαCGRP or hAM in modified Krebs-Ringer-HEPES medium (10), after which they were washed twice more with ice-cold PBS and harvested with 0.5 M NaOH. The associated cellular radioactivity was measured in a γ-counter. Specific binding was defined as the difference between total binding and nonspecific binding.

cAMP Measurements—Transfectants in 24-well plates were incubated for 15 min at 37 °C in Hanks' buffer containing 20 mM HEPES, 0.2% bovine serum albumin, 0.5 mM 3-isobutyl-1-methylxanthine (Sigma), and the indicated concentrations of hαCGRP or hAM. The reaction mixture was then replaced with 20 mM HCl and 1 M acetic acid to extract the intracellular cAMP, after which the resultant extracts were lyophilized and stored at −30 °C until assayed. The cAMP concentrations were measured using our specific radioimmunoassay (1).

FACS Analysis of Receptor Internalization and Recycling—Following cotransfection of the indicated cDNAs into HEK-293 cells stably expressing hCRLR-GFP in 6-well plates, the cells were exposed to selected concentrations of hαCGRP or hAM in prewarmed serum-free Dulbecco's modified Eagle's medium containing 20 mM HEPES and 0.2% bovine serum albumin for the indicated periods (up to 2 h) at 37 °C. For receptor recycling studies, the cells were incubating for 60 min with the agonist plus 10 μg/ml cycloheximide and 10 μg/ml brefeldin A and then washed three times with prewarmed PBS. The medium was then replaced with prewarmed Dulbecco's modified Eagle's medium containing 20 mM HEPES, 10% fetal bovine serum, 10 μg/ml cycloheximide, and 10 μg/ml brefeldin A for the indicated periods (up to 4 h) at 37 °C. Internalization and recycling were stopped by adding ice-cold PBS, after which the cells were harvested, resuspended in ice-cold FACS buffer, and labeled with anti-V5 monoclonal antibody and fluorescein PE-conjugated rabbit anti-mouse secondary antibody. The cells were then subjected to flow cytometry and analyzed as described above.

mRNA Expression Measured by Real Time Quantitative PCR—Total RNAs were extracted from HEK-293 cells either untransfected or transfected as indicated using total RNA isolation reagent (Invitrogen). Thereafter, the target cDNAs were synthesized from the respective mRNAs by reverse transcription using SuperScript reverse transcriptase (Invitrogen). The expression of mRNAs encoding hNSF was assessed using real time quantitative PCR (Prism 7700 Sequence Detector, Applied Biosystems, Foster City, CA) with original oligonucleotide primers (sense, 5′-AGAACAGTGACCGCACACCAT-3′; antisense, 5′-TCCACAACCACACAACTGAGC-3′) and a fluorescently labeled probe (5′-AGCGTGCTTCTGGAAGGCCCTCCTCACAGT-3′). The size of the amplified DNA was 223 bp. The levels of hNSF mRNA were normalized to those of glyceraldehyde-3-phosphate dehydrogenase mRNA, which served as an internal control.

Western Analysis—Following transient transfection of hNSF into cells plated in 6-well plates, the transfectants were washed twice with ice-cold PBS, harvested in 1 ml of sample buffer (28), and boiled for 10 min. Equal aliquots of protein (20 μg) were then subjected to 10% SDS gel electrophoresis and transferred to a Hybond-P membrane (Amersham Biosciences). The membrane was then blocked with 5% block reagent (Amersham Biosciences), washed, and incubated first for 1 h at room temperature with rabbit anti-hNSF antibody (1:1,000 dilution) and then with secondary antibody (1:10,000 dilution). hNSF proteins were detected using an ECL Plus chemiluminescence kit (Amersham Biosciences), after which they were quantitated by densitometry using Image Gauge (LAS-1000; Fujifilm).

Statistical Analysis—Results are expressed as means ± S.E. of at least three independent experiments. Differences between two groups were evaluated using Student's *t* tests; differences among multiple groups were evaluated with a one-way analysis of variance followed by Scheffe's tests. Values of $p < 0.05$ were considered significant.

RESULTS

Deletion of hRAMP C-tails—We previously established HEK-293 cells stably expressing hCRLR-GFP alone or together with Myc-hRAMPs and used them to visualize the cellular localization and trafficking of hCRLR (10). Following AM exposure, hCRLR is rapidly internalized together with its associated hRAMP, and then both are trafficked to lysosomes; fusion of GFP to the C terminus of hCRLR had no apparent effect on the trafficking of the heterodimeric receptor. In the present study, therefore, we used HEK-293 cells stably expressing hCRLR-GFP to examine the functions of the C-tails of the three hRAMPs within the respective CRLR/RAMP heterodimers.

We initially tested the effect of completely deleting the C-tails of the three V5-epitope tagged hRAMPs (Fig. 2). When coexpressed with hCRLR, V5-RAMP1, -2, and -3 were detected at the surfaces of 45.9, 21.9, and 38.9% of cells, respectively. On the other hand, the V5-RAMP deletion mutants Δ139-RAMP1, Δ166-RAMP2, and Δ139-RAMP3 appeared at the surface of 43.7, 5.0, and 38.8% of cells, respectively. Thus, deletion of the C-tail significantly reduced surface delivery of only RAMP2. Surface immunoreactivity was detected in only 0.55% of cells expressing the empty vector (Mock), which is well within the 2% limit of resolution characteristic of FACS analysis.

We next evaluated the binding profiles of ^{125}I-[Tyr^0]hαCGRP and ^{125}I-hAM to cells expressing each of the wild-type and mutant receptors (Fig. 3, *A* and *B*). When CRLR-GFP was coexpressed with empty vector (*Mock*), the cells showed only very low levels of specific binding of ^{125}I-[Tyr^0]αCGRP and ^{125}I-AM. Co-transfection of RAMP1 led to markedly higher specific ^{125}I-[Tyr^0]αCGRP binding than was seen with Δ139-RAMP1 (Fig. 3*A*), although there was no difference in the surface expression of either heterodimeric receptor (Fig. 2). Likewise, cotransfection of RAMP2 significantly increased the specific binding of

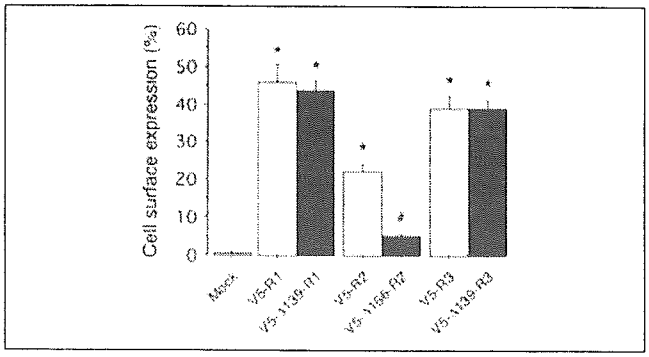

FIGURE 2. **FACS analysis of HEK-293 cells coexpressing hCRLR with intact hRAMP or a C-terminal deletion mutant.** HEK-293 cells stably expressing CRLR-GFP were transiently transfected with empty vector (*Mock*) or the indicated V5-RAMP or deletion mutant. The cells were incubated first with an anti-V5 monoclonal antibody and then with a fluorescein PE-conjugated rabbit anti-mouse secondary antibody. Samples incubated with only secondary antibody served as the control. Cell surface expression of each construct was estimated by flow cytometry. The *bars* represent means ± S.E. of six independent experiments. *, $p < 0.001$ *versus* control (*Mock*); #, $p < 0.02$ *versus* corresponding wild-type V5-RAMP.

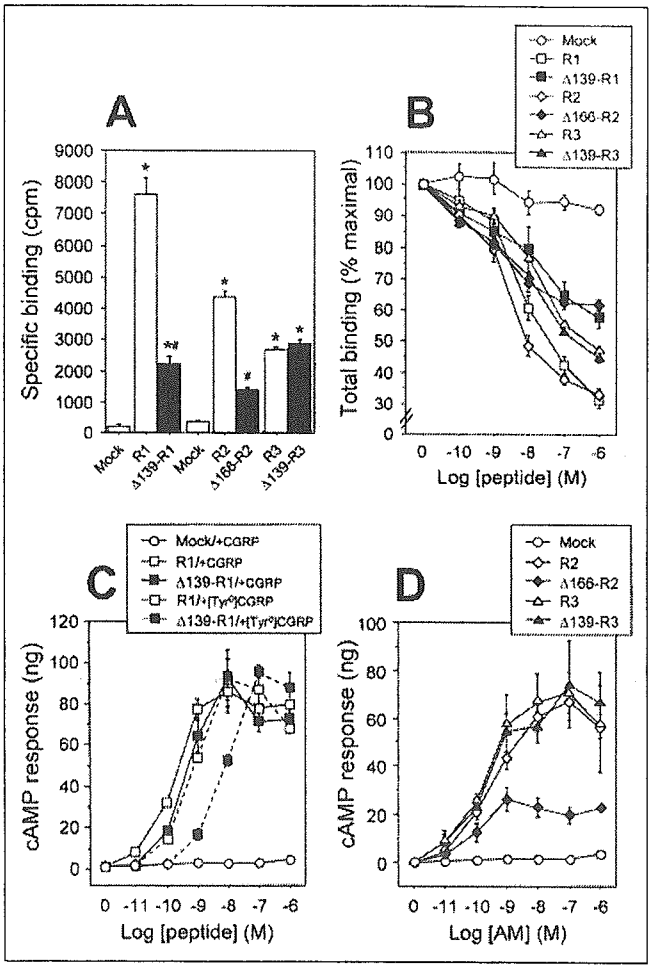

FIGURE 3. **Effects of hRAMP C-terminal deletion on agonist binding and evoked cAMP production in HEK-293 cells stably expressing hCRLR.** *A*, specific binding of ^{125}I-haCGRP and ^{125}I-hAM. HEK-293 cells expressing CRLR-GFP were transiently transfected with empty vector (*Mock*) or the indicated V5-RAMP or deletion mutant, after which the cells were incubated for 5 h at 4 °C with ^{125}I-αCGRP (100 pM) or ^{125}I-AM (20 pM) in the presence or absence of 1 μM unlabeled αCGRP or AM. *Bars* represent means ± S.E. of three experiments. *, $p < 0.002$ *versus* Mock; #, $p < 0.001$ *versus* corresponding wild-type V5-RAMP. *B*, displacement of radioligand. Cells were transfected and radiolabeled as in *A* either alone or with the indicated concentration of unlabeled ligand (αCGRP or AM). *Bars* represent means ± S.E. of three experiments. *C* and *D*, evoked cAMP production. After transient transfection of V5-RAMPs and the corresponding deletion mutants, cells were exposed to the indicated concentrations of αCGRP, [Tyr^0]αCGRP, or AM for 15 min at 37 °C and then lysed. The resultant lysates were analyzed for cAMP content. *Bars* represent means ± S.E. of three experiments.

^{125}I-AM to CRLR-GFP-expressing cells, whereas cotransfection of Δ166-RAMP2 did not. In this case, the reduced binding could be due to reduced surface delivery of the mutant receptors (Fig. 2). Finally, deletion of the RAMP3 C-tail had no effect on specific ^{125}I-AM binding.

Fig. 3*B* shows a set of ^{125}I-[Tyr^0]αCGRP and ^{125}I-AM competition curves for the wild-type and mutant receptors. The IC_{50} values derived from the curves obtained with cotransfection of Δ139-RAMP1 or Δ166-RAMP2 were both >1000 nM, which is much higher than those for RAMP1 and -2 (43.0 and 12.2 nM, respectively). By contrast, the IC_{50} values obtained with expression of RAMP3 or Δ139-RAMP3 were within the same order of magnitude (560 and 257 nM, respectively).

We then further characterized the mutant receptors by measuring agonist-induced intracellular cAMP accumulation (Fig. 3, *C* and *D*). αCGRP and AM elicited little or no cAMP production in HEK-293 cells expressing CRLR-GFP alone, indicating that the stable transfectants used in this study express no functional RAMP proteins. In cells coexpressing RAMP1 and CRLR-GFP, by contrast, αCGRP (EC_{50} = 0.18 nM) elicited marked increases in cAMP (Fig. 3*C*). In cells expressing Δ139-RAMP1 with CRLR-GFP, the EC_{50} for αCGRP was increased only a little, as compared with RAMP1 (to 0.49 nM), and the maximal responses were also similar to those seen with RAMP1 (Fig. 3*C*). Interestingly, the responses to [Tyr^0]αCGRP by cells expressing CRLR-GFP/Δ139-RAMP1 (EC_{50} = 8.5 nM) were significantly smaller than those seen in cells expressing CRLR-GFP/RAMP1 (EC_{50} = 0.79 nM). In cells transfected with RAMP2, AM elicited significant increases in cAMP (EC_{50} = 0.38 nM), but these responses were diminished by 62.1% in cells transfected with Δ166-RAMP2, although there was no significant change in EC_{50} (0.16 nM) (Fig. 3*D*). AM-evoked cAMP production did not significantly differ in cells expressing RAMP3 or Δ139-RAMP3 (EC_{50} = 0.41 and 0.20 nM, respectively) (Fig. 3*D*). That the cAMP production elicited via the respective receptors largely paralleled the profile of radioligand binding (Fig. 3, *A* and *B*) suggests that the C-tails of RAMP1 and -3 have little or no involvement with agonist binding and signaling.

We previously quantified the internalization and recycling of AM receptors (CRLR/RAMP heterodimers) using radioligand binding assays; however, interpretation of those experiments was complicated by the high degree of nonspecific AM binding, which reflected the highly hydrophobic and basic nature of the native peptide (1, 10, 11). In the present study, therefore, we used FACS to evaluate agonist-mediated internalization and recycling of wild-type and mutant CRLR-GFP/RAMP heterodimers. Fig. 4*A* shows the receptor internalization induced by 1 μM αCGRP- or AM. Exposure to the appropriate agonist elicited rapid declines in cell surface expression of wild-type CRLR-GFP/RAMP1 and -3 that led to 40–60% reductions in signal strength within 2 h and to 90% reduction in cell surface CRLR-GFP/RAMP2 within 30 min. Heterodimers composed of CRLR-GFP plus Δ139-RAMP1 or Δ166-RAMP2 tended to be internalized somewhat less efficiently, whereas internalization of the CRLR-GFP/Δ139-RAMP3 heterodimer was markedly enhanced. Notably, these phenomena occurred with no changes in cell surface CRLR-GFP expression or AM binding and signaling (Figs. 2 and 3).

The dose dependence of the agonist-evoked receptor internalization is illustrated in Fig. 4*B*. αCGRP elicited equivalent dose-dependent internalization of CRLR-GFP/RAMP1 and CRLR-GFP/Δ139-RAMP1. AM dose-dependently induced RAMP2-mediated internalization of CRLR-GFP, which was more efficient than RAMP1-mediated internalization. And Δ166-RAMP2 mediated internalization of CRLR-GFP even more efficiently than did wild-type RAMP2, although the basal surface expression of CRLR-GFP/Δ166-RAMP2 was much lower (Fig. 2*A*). Δ139-RAMP3-mediated internalization of CRLR-GFP only differed from that mediated by wild-type RAMP3 at high AM concentrations (100 nM and 1 μM), at which time internalization of the mutant was more efficient.

Progressive Truncation of the C-Tails of hRAMP2 and -3—The results presented so far show that for hRAMP1, the C-tail is not necessary for cell surface delivery and internalization of CRLR (Figs. 2 and 4). For hRAMP2 and -3, by contrast, the respective C-tails do appear to be involved in determining the surface expression and internalization kinetics of CRLR.

To determine more precisely which sites on the C-tails of hRAMP2 and -3 regulate the cellular trafficking of CRLR/RAMP heterodimers, we constructed a group of progressive C-tail truncation mutants (Fig. 1) and then transfected each RAMP construct into HEK-293 cells stably expressing CRLR-GFP. When Δ166- or Δ167-RAMP2 was individually transfected into HEK-293 cells, its transfection efficiency (~15%) was

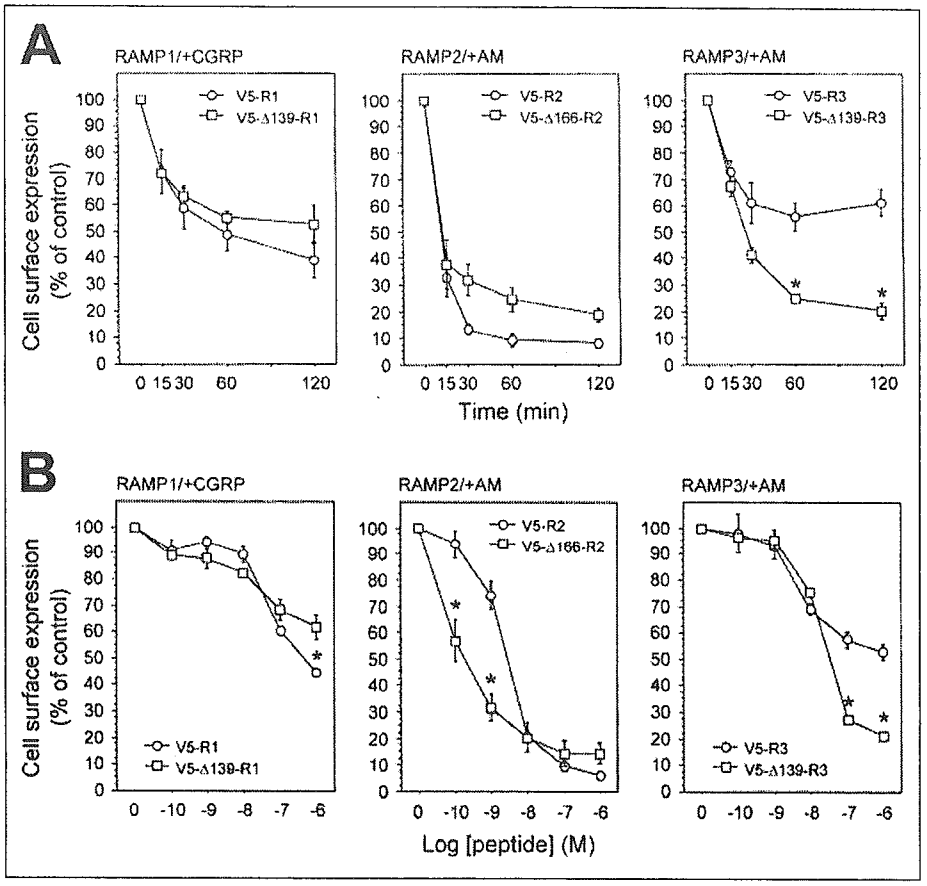

FIGURE 4. **FACS analysis of the time course of agonist-induced internalization of hCRLR with hRAMPs or their C-terminal deletion mutants.** *A*, time-dependent loss of surface CRLR/RAMP heterodimers. HEK-293 cells stably expressing CRLR-GFP were transiently transfected with V5-RAMPs or their C-terminal deletion mutants and then treated with 1 μM αCGRP or AM for the indicated times. Cell surface expression of each construct was estimated by flow cytometry. The *symbols* represent means ± S.E. of three independent experiments; *, $p < 0.006$ *versus* control. *B*, agonist-evoked internalization of hCRLR with hRAMPs or their deletion mutants. Each transfectant was incubated for 60 min with the indicated concentrations of αCGRP or AM. Cell surface expression of each construct was estimated by flow cytometry. *Symbols* represent means ± S.E. of three independent experiments; *, $p < 0.03$ *versus* control.

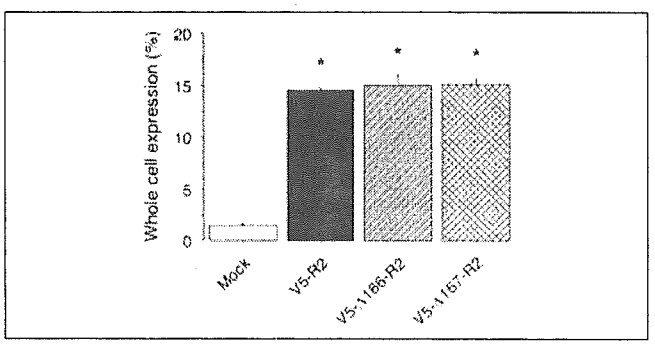

FIGURE 5. **FACS analysis of whole cell expression of hRAMP2 and its truncation mutants.** The indicated RAMP constructs were transiently transfected into HEK-293 cells. Forty-eight hours after transfection, cells were permeabilized with IntraPrep™ reagent and then incubated for 15 min at room temperature with anti-V5-FITC antibody; mock incubation with the antibody served as the control. Whole cell expression of each construct was estimated by flow cytometry. The *symbols* represent means ± S.E. of three independent experiments; *, $p < 0.001$ *versus* control.

comparable with that for wild-type RAMP2 (Fig. 5). Moreover, immunocytochemical analysis showed that almost all of both mutants remained in the ER, representing a pool of newly synthesized molecules not yet transported to the cell surface (Fig. 6). Although they were transfected into CRLR-GFP-expressing cells, however, Δ166- and Δ167-RAMP2 largely failed to transport CRLR-GFP to the cell surface, resulting in significant reductions in specific ^{125}I-AM binding and AM-evoked cAMP production (Table 1). This suggests that the 168th and 169th amino acids (SK sequence) of RAMP2 are important for cell surface delivery of CRLR. The reason for the discrepancy between the IC_{50} and EC_{50} remains unclear, however. By contrast, Δ168- and Δ169-RAMP mediated substantially greater levels of cell surface CRLR-GFP expression, so that AM binding and signaling were equivalent to that seen with wild-type RAMP2 (Table 1). All of the RAMP3 truncation mutants appeared together with CRLR-GFP at the cell surface (Fig. 6*A*), and the resultant receptors showed AM binding and signaling that was comparable with that seen with wild-type RAMP3 (Table 1).

Among the RAMP2 mutants, Δ166 significantly reduced internalization of CRLR-GFP (Fig. 7). Conversely, the Δ139- and Δ140-RAMP3 mutants mediated significantly greater CRLR-GFP internalization than wild-type RAMP3 (Fig. 7). Such increases were not seen with Δ141-RAMP3, and CRLR-GFP internalization mediated by Δ142, Δ143, and Δ144 was equal to that seen with wild-type RAMP3. Thus, the presence of amino acids 141 and 142 (SK sequence) of RAMP3 leads to significant decreases in CRLR internalization.

Characteristics of hRAMP C-tail Chimeras—The SK sequence is highly conserved in the C-tails of all three hRAMPs (Fig. 1) as well as in RAMP isoforms from other species (17). We therefore tested whether exchanging C-tails would affect the cellular trafficking of CRLR-GFP. Given that hRAMP2 promoted CRLR internalization more effectively than other hRAMP isoforms did and that there were no differences in CRLR surface delivery and internalization by hRAMP1 and -3, we constructed four RAMP chimeras (RAMP1/2, -2/1, -2/3, and -3/2) by taking advantage of unique restriction sites that enabled us to generate four hybrid genes. These RAMP chimeras were then transiently transfected into HEK293 cells stably expressing CRLR-GFP and characterized by FACS analysis. As shown in Table 2, cell surface expression and evoked CRLR-GFP internalization of all four chimeras was comparable with

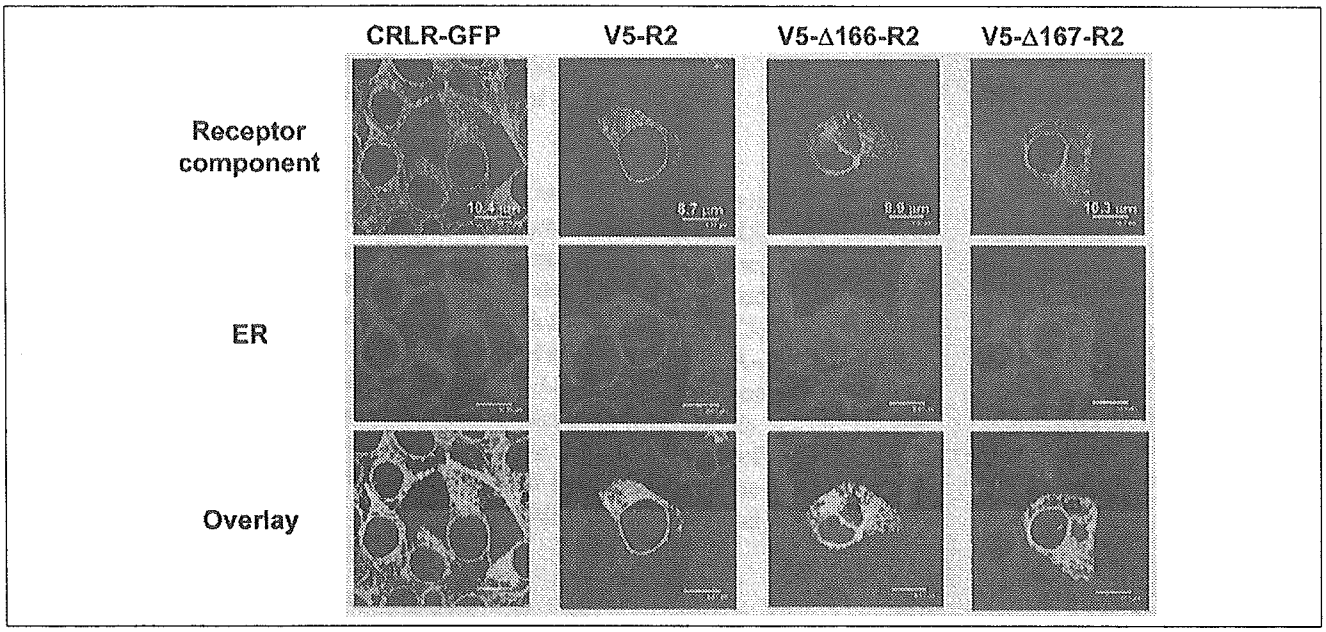

FIGURE 6. **Intracellular localization of V5-hRAMP2 and its truncation mutants.** The indicated RAMP2 constructs were transiently transfected into HEK-293 cells, after which their subcellular distribution was assessed by confocal microscopy in permeabilized cells using anti-V5-FITC antibody. Calnexin (for the ER) was visualized using the appropriate secondary antibody (Alexa Fluor® 594). Co-localization with the ER marker was determined by overlay of the images (*lower panels*). HEK-293 cells stably expressing CRLR-GFP served as the control for co-localization of CRLR-GFP and the ER (*left panels*). *Bar*, ~10 μm.

TABLE 1

Characterization of HEK-293 cells expressing CRLR-GFP and progressive V5-RAMP2 and -3 truncation mutants

The indicated RAMP constructs were transiently transfected into CRLR-GFP-expressing HEK-293 cells. Surface expression of each construct was estimated by flow cytometry. The results represent the means ± S.E. of three independent experiments.

	Cell surface expression (% V5-RAMP2 or -3)	^{125}I-AM binding		AM-evoked cAMP production	
		IC_{50}	Specific binding (% V5-RAMP2 or -3)	EC_{50}	Maximal responses (% V5-RAMP2 or -3)
	%	nM	%	nM	%
V5-RAMP2 (R2)	100	12.2 ± 5.0	100	0.38 ± 0.14	100
V5-Δ166-R2	14.6 ± 1.5[a]	>1000	31.8 ± 1.4[a]	0.16 ± 0.07	37.9 ± 4.7[a]
V5-Δ167-R2	29.0 ± 2.3[a]	>1000	48.0 ± 2.9[a]	0.21 ± 0.09	52.3 ± 1.8[a]
V5-Δ168-R2	61.7 ± 5.5	13.7 ± 5.3	98.4 ± 7.2	0.26 ± 0.22	73.8 ± 20.5
V5-Δ169-R2	83.6 ± 7.8	12.9 ± 3.5	95.8 ± 3.9	0.10 ± 0.06	87.8 ± 19.3
V5-Δ172-R2	55.9 ± 8.1	18.0 ± 6.0	83.1 ± 2.4[a]	0.24 ± 0.04	61.5 ± 4.9
V5-RAMP3 (R3)	100	560 ± 100	100	0.41 ± 0.25	100
V5-Δ139-R3	89.3 ± 6.0	257 ± 49	107 ± 4.3	0.20 ± 0.08	93.8 ± 12.1
V5-Δ140-R3	79.7 ± 5.3	687 ± 70	93.9 ± 1.7	2.50 ± 1.49	91.0 ± 5.7
V5-Δ141-R3	89.1 ± 11.6	317 ± 73	114 ± 1.3[a]	0.30 ± 0.14	116 ± 7.5
V5-Δ142-R3	79.4 ± 9.7	483 ± 193	114 ± 4.5	0.98 ± 0.31	101 ± 8.6
V5-Δ143-R3	84.0 ± 12.8	386 ± 307	111 ± 11.4	0.38 ± 0.21	113 ± 21.6
V5-Δ144-R3	78.2 ± 10.3	383 ± 105	114 ± 6.1	0.13 ± 0.09	102 ± 12.1

[a] $p < 0.03$ *versus* corresponding control (V5-RAMP2 or -3).

that seen with the respective wild-type RAMPs. Thus, exchanging C-tails did not affect RAMP-mediated surface delivery or internalization of CRLR.

Effect of hRAMP C-tail Deletion on Receptor Recycling—For recycling studies, cells were pretreated with 10 μg/ml cycloheximide and 10 μg/ml brefeldin A to respectively inhibit *de novo* protein synthesis and cause disassembly of the Golgi apparatus (29); neither of these reagents had any effect of their own on CGRP- or AM-induced internalization of CRLR-GFP/RAMPs (data not shown). Subsequent treatment of cells with 1 μM αCGRP or AM for 60 min elicited a loss of cell surface receptors that persisted for at least 2 h after washing out the ligands (Fig. 8*A*). Very similar results were seen with Δ139-RAMP1, Δ166-RAMP2, and Δ139-RAMP3, suggesting the RAMP C-tails are not involved in lysosomal sorting of CRLR or the binding of protein(s) that determine the fate of internalized receptors.

Internalization and Recycling of AM_2 Receptors in Cells Cotransfected with hNSF—It was recently shown that, unlike NHERF, NSF contains no recognizable PDZ domains (30) but nonetheless interacts with the PDZ motif of hRAMP3, enabling internalized AM_2 receptors to undergo slow recycling (18). Conversely, NSF enhances β-arrestin 1-mediated β_2-AR internalization (31). Notably, although rat and mouse RAMP3 C-tails contain a RLL sequence instead of a PDZ motif, NSF also promotes recycling of these CRLR/RAMP3 heterodimers (18). With the aim of better understanding the role of NSF in AM_2 receptor trafficking, in the present study, we tested whether the reported effects of hNSF on CRLR/RAMP3 trafficking are reproduced in HEK-293 cells endogenously expressing hNSF and in hNSF transfectants.

We first confirmed that NSF was indeed endogenously expressed in HEK-293 cells by identifying both NSF mRNA and protein in the

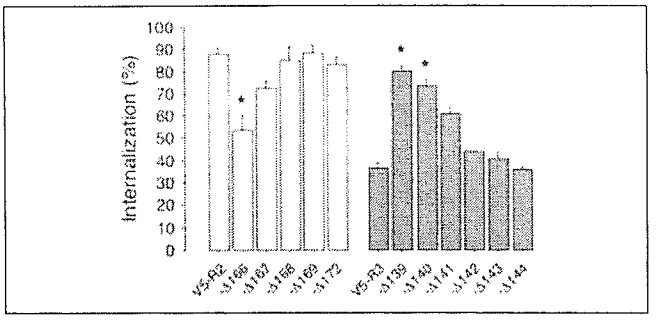

FIGURE 7. **FACS analysis of internalization of hCRLR with progressive hRAMP2 and -3 truncation mutants.** The indicated RAMP constructs were transiently transfected into CRLR-GFP-expressing HEK-293 cells. Surface expression of each construct was estimated by flow cytometry before and after exposing cells to 1 μM AM for 60 min. The results represent the means ± S.E. of three independent experiments; *, $p < 0.003$ *versus* corresponding control (V5-RAMP2 or -3).

TABLE 2

FACS analysis of cell surface delivery and internalization of CRLR-GFP and V5-RAMP chimeras in which the C-tails were exchanged among the three RAMPs

The indicated V5-RAMPs or their chimeras were transiently transfected into CRLR-GFP-expressing HEK-293 cells. Surface expression of each construct was estimated by flow cytometry before and after exposing cells to 1 μM αCGRP or AM for 60 min. The results represent the means ± S.E. of three independent experiments.

	Cell surface expression	Internalization
	%	%
V5-RAMP1	51.8 ± 3.7	50.0 ± 4.3
V5-RAMP2	23.2 ± 2.7	94.5 ± 1.6
V5-RAMP3	46.3 ± 4.8	35.5 ± 1.8
V5-RAMP1/2	49.7 ± 5.6	53.7 ± 7.2
V5-RAMP2/1	25.8 ± 2.3	91.8 ± 0.4
V5-RAMP2/3	19.5 ± 1.4	88.2 ± 1.2
V5-RAMP3/2	44.9 ± 6.1	36.7 ± 3.8

cells (Fig. 8, *B* and *C*). Thereafter, we determined that the levels of the transcript were unaffected by transfection of CRLR-GFP alone or together with V5-RAMP3 (Fig. 8*D*). When NSF was transfected into otherwise untransfected HEK-293 cells and into CRLR-GFP transfectants, levels of its transcript were markedly higher than their endogenous levels in both (Fig. 8*B*). In those cases, Western analysis of NSF protein yielded a single, strong 76-kDa band that was identical to the band obtained when endogenous NSF was probed (Fig. 8*C*), which confirmed that our NSF transfection system worked appropriately. Exposure to 10 nM or 1 μM AM for 60 min induced a rapid decline in cell surface CRLR-GFP/V5-RAMP3 that persisted for at least 4 h after washing out the AM (Fig. 8*D*). Cotransfection of NSF had no effect on these internalization kinetics, and recycling of CRLR/RAMP3 heterodimers, if it occurred, was highly inefficient, even in the presence of abundant NSF (Fig. 8*D*).

DISCUSSION

Since their discovery, there have been only a few reports addressing the functions of the respective C-tails of the three RAMP isoforms (17–19, 32, 33); more extensively studied have been their extracellular domains (11–13, 17, 32, 34, 35). Consequently, whereas nearly all highly conserved residues are known to play key roles in the function and trafficking of cell surface receptors, nothing is known about the functions of the highly conserved Ser and Lys resides within RAMP C-tails. In the present study, we showed that deleting the C-tail from RAMP3 (Δ139-RAMP3) significantly enhanced AM-induced CRLR-GFP internalization but did not affect the targeting of CRLR-GFP to the cell surface or AM binding and signaling. It is therefore unlikely that the truncation of RAMP3 promoted AM-induced conformational changes in the heterodimeric receptors that would alter the binding of AM and/or the interaction of the receptor with G proteins. On the other hand, like wild-type RAMP3, all of the tested RAMP3 truncation mutants that contained the SK sequence (Δ142-, Δ143-, and Δ144-RAMP3) mediated CRLR-GFP internalization less efficiently than those that did not (Δ139-, Δ140-, or Δ141-RAMP3). We also found that substituting the RAMP3 C-tail with the RAMP2 C-tail, which also contains a SK sequence, had no effect on the AM-induced CRLR-GFP internalization. Taken together, these results suggest that the SK sequence participates in the negative regulation of CRLR/RAMP3 internalization.

The Ser/Thr residues present in the C-tails of the three RAMP have been thought to be potential phosphorylation sites, but Hilairet *et al.* (6) showed that in HEK-293 cells overexpressing CRLR/RAMP heterodimers, agonists rapidly promote phosphorylation of CRLR but not RAMP. They also demonstrated that internalization of the heterodimeric receptors was dependent on β-arrestins (6). In the present study, complete removal of the respective RAMP C-tails did not diminish the maximal extent of internalization. It therefore seems unlikely that β-arrestins interact with the RAMP C-tails.

Similar in function to the SK sequence, a dileucine (LL) motif, which is conserved among GPCRs (36), is also present in the C-tail of RAMP3. This motif negatively regulates lutropin/choriogonadotropin receptor (LHR) internalization, since leucine-to-alanine mutations increased the agonist-stimulated internalization of the receptor (37). It is thought that the LL motif participates in protein sorting through direct interaction with two clathrin adaptor protein (AP) complexes, AP-1 and AP-2 (38–40), and the point mutations disrupted the interaction of the LHR with AP-2 at the plasma membrane (39). On the other hand, these mutations are believed to enhance the binding of β-arrestins to the LHR, thereby promoting bridge formation between β-arrestins and clathrin (37). We suggest that, instead of β-arrestins, the RAMP3 C-tail may interact with other intracellular proteins similar to LRP6, another GPCR accessory protein that interacts with axin and catinin (41).

We believe it is noteworthy that the hRAMP3 C-tail contains not only a LL sequence but also a type I PDZ binding sequence (see Fig. 1). Recently, NHERF-1 was found to interact with the PDZ motif of hRAMP3, resulting in complete inhibition of CRLR/RAMP3 internalization (33). In that case, NHERF-1 is thought to act by tethering surface AM_2 receptors to the actin cytoskeleton in a manner also seen with epidermal growth factor receptors (42). By contrast, NHERF-1 promotes the agonist-mediated recycling of β_2-ARs, which also have a PDZ motif (SLL) (30). The mechanism by which NHERF-1 exerts these differing effects on different GPCRs remains unknown. In the present study, three RAMP3 truncation mutants (Δ142-, Δ143-, and Δ144-RAMP3) and the RAMP3/2 chimera, all of which lack both the LL and PDZ sequences, failed to enhance the AM-induced CRLR-GFP internalization. However, this does not preclude the possibility that the level of endogenous NHERF-1 expression in HEK-293 cells used was insufficient to modulate the behavior of the overexpressed RAMP3.

We also showed that deleting the C-tail of RAMP2 impaired the targeting of the CRLR-GFP to the cell surface, thereby markedly reducing AM binding and signaling. Most of the newly synthesized Δ166-RAMP2 remained in the ER along with CRLR-GFP. By contrast, removing the C-tail from RAMP1 or -3 did not diminish surface delivery of the respective receptors. All of the RAMP2 mutants containing an SK sequence (Δ168-, Δ169-, and Δ172-RAMP2) showed better surface CRLR-GFP expression than was seen with Δ166-RAMP2, which lacked the SK sequence. Apparently, the SK sequence in the RAMP2 C-tail is involved in the proper membrane localization of the CRLR/RAMP2. To our knowledge, there have

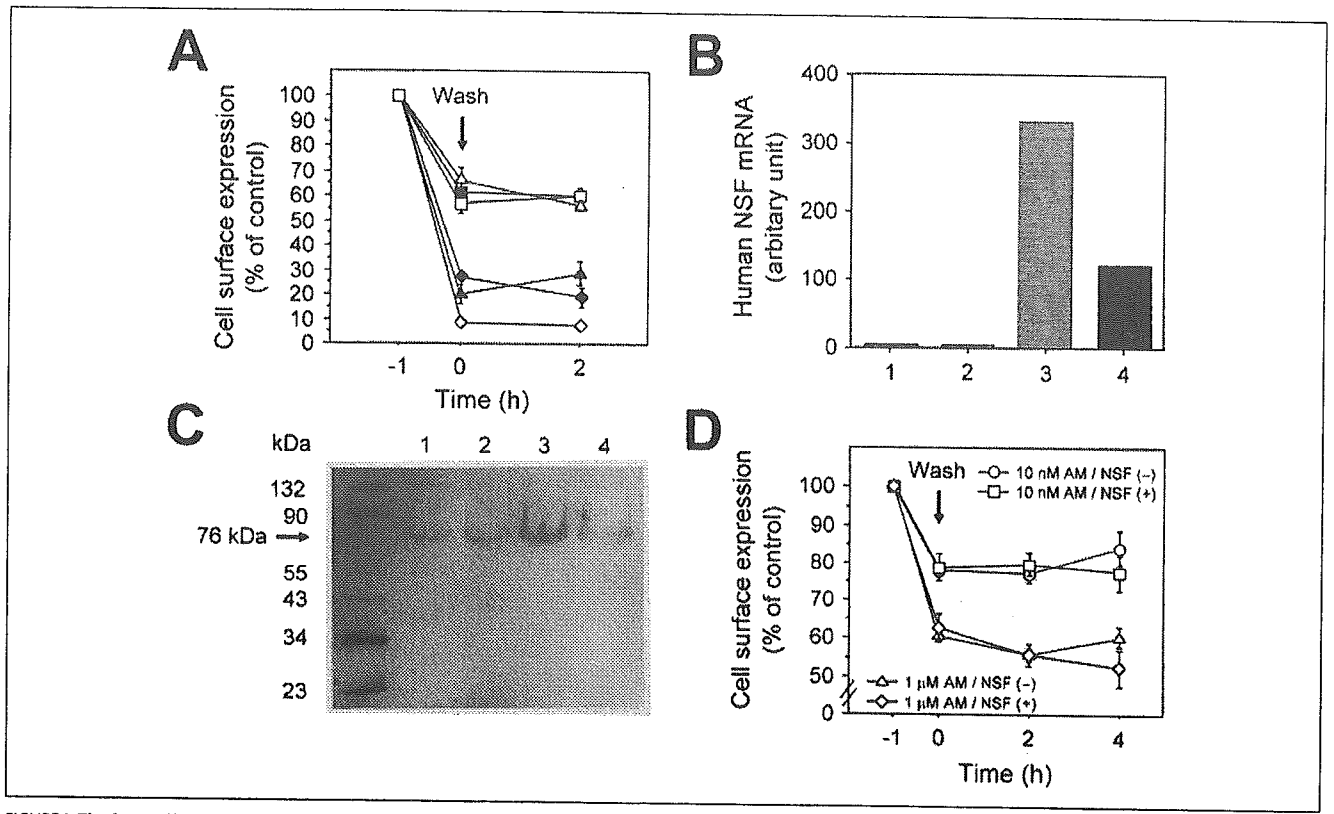

FIGURE 8. **The fates of internalized hCRLR and hRAMPs and their C-terminal deletion mutants.** *A*, FACS analysis of recycling of the internalized heterodimeric receptors. HEK-293 cells stably expressing CRLR-GFP were transiently transfected with each RAMP construct (*symbols* are the same as in Fig. 3*B*), after which they were incubated for 60 min with 1 μM αCGRP or AM plus 10 μg/ml cycloheximide and 10 μg/ml brefeldin A. The cells were then washed with prewarmed PBS and labeled with the indicated antibodies. Cell surface expression of each construct was estimated by flow cytometry. *Bars* represent means ± S.E. of three independent experiments. *B*, endogenous and transiently transfected hNSF mRNA levels. *1*, intact HEK-293 cells; *2*, HEK-293 cells stably expressing CRLR-GFP; *3*, NSF-transfected HEK-293 cells; *4*, NSF-transfected HEK-293 cells stably expressing CRLR-GFP. Expression of NSF mRNA was assessed using real time quantitative PCR with the appropriate primers and probes. Levels of NSF mRNA were normalized to that of GAPDH mRNA, which served as an internal control. *Bars* represent the average of two experiments. *C*, Western analysis of endogenous NSF and overexpressed NSF in HEK-293 cells. Equal aliquots of protein (20 μg) were subjected to 10% SDS gel electrophoresis. *Lane 1*, cells expressing empty vector (*Mock*); *lane 2*, cells stably expressing CRLR-GFP; *lane 3*, cells transiently expressing NSF; *lane 4*, cells expressing both CRLR-GFP and NSF. The blots shown are representative of three independent experiments. *D*, FACS analysis of the recycling of CRLR and RAMP3 in the presence and absence of NSF. CRLR-GFP-expressing cells were transiently transfected with V5-RAMP3 plus empty vector or NSF, after which they were incubated for 60 min with 10 nM or 1 μM AM plus 10 μg/ml cycloheximide and 10 μg/ml brefeldin A. The cells were then treated as described in *A*. Cell surface expression of each construct was estimated by flow cytometry. The *symbols* represent means ± S.E. of three independent experiments.

been no studies on the relation between the SK sequence and surface delivery of other GPCRs, but the LL sequence in the C-tail of the V_2 vasopressin receptor was found to be crucial for ER-to-Golgi transfer of that receptor, presumably by helping establish a correct and transport-competent folding state (36). Similarly, RAMPs appear to mediate transport of the CRLR from the ER to the Golgi, since CRLR was restricted to the ER in the absence of RAMPs (6). It therefore seems likely that the SK sequence in the RAMP2 C-tail, but not that in the RAMP3 C-tail, is essential for the escape of CRLR from the ER. The mechanism underlying the differential effect of the SK sequence on the cellular trafficking of these two AM receptors remains to be determined.

There have been two studies on the effects of CGRP in HEK-293 cells coexpressing hCRLR with a hRAMP1 C-tail deletion mutant (19, 32). One found that the C-tail deletion resulted in a 1-order of magnitude reduction in CGRP-stimulated cAMP formation, but no data on CGRP binding were shown (19). In that case, the 140th residue Gln, but not the SK sequence, most likely determined the affinity of CGRP for the receptor. The other study found no significant changes in CGRP binding or signaling (32). Similarly, we found that deleting the C-tail of RAMP1 had little effect on receptor signaling, as reflected by CGRP-evoked cAMP production, although the binding profile we obtained differed from that obtained in the earlier study (32). This absence of a significant change in the potency of CGRP may indicate that there was little change in the internalization of CRLR-GFP. In contrast to the αCGRP responses, ^{125}I-[Tyr^0]αCGRP binding to CRLR-GFP/Δ139-RAMP1 was much diminished. This discrepancy could be due in part to interference by the extra N-terminal tyrosine residue (Tyr^0). In any event, the contribution of the RAMP1 C-tail to CGRP potency is much smaller than that made by its extracellular domain (13, 17, 32, 34, 35).

Several earlier studies showed that internalized CRLR/RAMP heterodimers are trafficked to lysosomes for degradation (6, 10). It is now recognized that receptor ubiquitination is essential for proper trafficking to lysosomes (43). Indeed, our CRLR-GFP-transfected HEK-293 cells abundantly expressed endogenous ubiquitin, which attaches to lysine residues within the substrate proteins (data not shown). Nevertheless, truncation of RAMP C-tails that removed the Lys residues failed to promote recycling of CRLR-GFP. This raises the possibility that expression of intracellular proteins involved in mediating appropriate receptor recycling was inadequate in the HEK-293 cells used. NSF, like NHERF, is believed to enhance recycling of internalized receptors (44), and it was recently shown that NSF interacts with the PDZ motif of hRAMP3, enabling internalized AM_2 receptors to undergo slow recycling (18). Notably, although rat and mouse RAMP3 tails contain an RLL sequence instead of a PDZ motif, NSF also promoted recycling of CRLR/RAMP3 heterodimers

(18). In the present study, however, the cells abundantly expressed endogenous NSF, making it unlikely that poor expression of NSF underlies the trafficking of CRLR-GFP/RAMP3 to lysosomes without recycling. Even overexpression of NSF in these cells did not alter the AM-mediated trafficking of AM_2 receptors.

The rapid recycling pathway has been best studied and characterized for the β_2-AR, which has a PDZ motif in its C-tail (14, 15, 30) and which requires both NHERF and NSF for its recycling (30, 44). Indeed, among 59 representative seven-transmembrane segment GPCRs tested, NSF bound most strongly to the β_2-AR tail (44). However, a point mutation within the PDZ motif that disrupted the binding of NSF, but not that of NHERF, had no effect on β_2-AR recycling (30). In addition, the β_1-AR and cystic fibrosis transmembrane regulator each contain a C-terminal PDZ binding sequence (SKV and TRL, respectively) and undergo rapid recycling, despite their failure to bind NSF (30). Thus, NSF binding to GPCRs and RAMP3 is not required for recycling of proteins containing PDZ binding sequences.

In summary, our results indicate that the C-tails of hRAMP2 and -3 are involved in hCRLR surface delivery and internalization, respectively, and that the highly conserved SK sequence within their C-tails is a key determinant of the cellular behavior of the AM_1 and AM_2 receptors.

REFERENCES

1. Kitamura, K., Kangawa, K., Kawamoto, M., Ichiki, Y., Nakamura, S., Matsuo, H., and Eto, T. (1993) *Biochem. Biophys. Res. Commun.* **192,** 553–560
2. Eto, T. (2001) *Peptides* **22,** 1693–1711
3. Poyner, D. R., Sexton, P. M., Marshall, I., Smith, D. M., Quirion, R., Born. W., Muff, R., Fischer, J. A., and Foord, S. M. (2002) *Pharmacol. Rev.* **54,** 233–246
4. McLatchie, L. M., Fraser, N. J., Main, M. J., Wise, A., Brown, J., Thompson, N., Solari, R., Lee, M. G., and Foord, S. M. (1998) *Nature* **393,** 333–339
5. Sexton, P. M., Albiston, A., Morfis, M., and Tilakaratne, N. (2001) *Cell Signal.* **13,** 73–83
6. Hilairet, S., Belanger, C., Bertrand, J., Laperriere, A., Foord, S. M., and Bouvier, M. (2001) *J. Biol. Chem.* **276,** 42182–42190
7. Kuwasako, K., Cao, Y-N., Nagoshi, Y., Kitamura, K., and Eto, T. (2004) *Peptides* **25,** 2003–2012
8. Nagoshi, Y., Kuwasako, K., Ito, K., Uemura, T., Kato, J., Kitamura, K., and Eto, T. (2002) *Eur. J. Pharmacol.* **450,** 237–243
9. Muff, R., Born, W., and Fischer, J. A. (2003) *Hypertens. Res.* **26,** 3–8
10. Kuwasako, K., Shimekake, Y., Masuda, M., Nakahara, K., Yoshida, T., Kitaura, M., Kitamura, K., Eto, T., and Sakata, T. (2000) *J. Biol. Chem.* **275,** 29602–29609
11. Kuwasako, K., Kitamura, K., Ito, K., Uemura, T., Yanagita, Y., Kato, J., Sakata, T., and Eto, T. (2001) *J. Biol. Chem.* **276,** 49459–49465
12. Kuwasako, K., Kitamura, K., Onitsuka, H., Uemura, T., Nagoshi, Y., Kato, J., and Eto, T. (2002) *FEBS Lett.* **519,** 113–116
13. Kuwasako, K., Kitamura, K., Nagoshi, Y., Cao Y-N., and Eto, T. (2003) *J. Biol. Chem.* **278,** 22623–22630
14. Koenig, J. A., and Edwardson, J. M. (1997) *Trends. Pharmacol. Sci.* **18,** 276–287
15. Krupnick, J. G., and Benovic, J. L. (1998) *Annu. Rev. Pharmacol. Toxicol.* **38,** 289–319
16. Ferguson, S. S. G. (2001) *Pharmacol. Rev.* **53,** 1–24
17. Hay, D. L., Poyner, D. R., and Sexton, P. M. (2006) *Pharmacol. Ther.* **109,** 173–197
18. Bomberger, J. M., Parameswaran, N., Hall, C. S., Aiyar, N., and Spielman, W. S. (2005) *J. Biol. Chem.* **280,** 9297–9307
19. Steiner, S., Muff, R., Gujer, R., Fischer, J. A., and Born, W. (2002) *Biochemistry* **41,** 11398–11404
20. Hicke, L., and Riezman, H. (1996) *Cell* **84,** 277–287
21. Roth, A. F., and Davis, N. G. (1996) *J. Cell Biol.* **134,** 661–674
22. Martin, N. P., Lefkowitz, R. J., and Shenoy, S. K. (2003) *J. Biol. Chem.* **278,** 45954–45959
23. Shenoy, S. K., and Lefkowitz, R. J. (2003) *J. Biol. Chem.* **278,** 14498–14506
24. Kuwasako, K., Cao, Y-N., Nagoshi, Y., Tsuruda, T., Kitamura, K., and Eto, T. (2004) *Mol. Pharmacol.* **65,** 207–213
25. Aiyar, N., Rand, K., Elshourbagy, N. A., Zeng, Z., Adamou, J. E., Bergsma, D. J., and Li, Y. (1996) *J. Biol. Chem.* **271,** 11325–11329
26. Guon, X.-M., Kobilka, T. S., and Kobilka, B. K. (1992) *J. Biol. Chem.* **267,** 21995–21998
27. Nagoshi, Y., Kuwasako, K., Cao, Y-N., Kitamura, K., and Eto, T. (2004) *Biochem. Biophys. Res. Commun.* **314,** 1057–1063
28. Cao, Y-N., Kuwasako, K., Kato, J., Yanagita, T., Tsuruda, T., Kawano, J., Nagoshi, Y., Chen, A. F., Wada, A., Suganuma, T., Eto, T., and Kitamura, K. (2005) *Biochem. Biophys. Res. Commun.* **332,** 866–872
29. Xu, J., and Tse, F. W. (1999) *J. Biol. Chem.* **274,** 19095–19102
30. Gage, R. M., Matveeva, E. A., Whiteheart, S. W., von Zastrow, M. (2005) *J. Biol. Chem.* **280,** 3305–3313
31. McDonald, P. H., Cote, N. L., Lin, F-T., Premont, R. T., Pitcher, J. A., and Lefkowitz, R. J. (1999) *J. Biol. Chem.* **274,** 10677–10680
32. Fitzsimmons, T. J., Zhao, X., and Wank, S. A. (2003) *J. Biol. Chem.* **278,** 14313–14320
33. Bomberger, J. M., Spielman, W. S., Hall, C. S., Weinman, E. J., and Parameswaran, N. (2005) *J. Biol. Chem.* **280,** 23926–23935
34. Fraser, N. J., Wise, A., Brown, J., McLatchie, L. M., Main, M. J., and Foord, S. M. (1999) *Mol. Pharmacol.* **55,** 1054–1059
35. Hilairet, S., Foord, S. M., Marshall, F. H., and Bouvier, M. (2001) *J. Biol. Chem.* **276,** 29575–29581
36. Schulein, R., Hermosilla, R., Oksche, A., Dehe, M., Wiesner, B., Krause, G., and Rosenthal, W. (1998) *Mol. Pharmacol.* **54,** 525–535
37. Nakamura, K., and Ascoli, M. (1999) *Mol. Pharmacol.* **56,** 728–736
38. Dietrich, J., Kastrup, J., Nielsen, B. L., Odum, N., and Geisler, C. (1997) *J. Cell Biol.* **138,** 271–281
39. Kirchhausen, T., Bonifacino, J. S., and Riezman, H. (1997) *Curr. Opin. Cell Biol.* **9,** 488–495
40. Rapoport, I., Chen, Y-C., Cupers, P., Shoelson, S. E., and Kirchhausen, T. (1998) *EMBO J.* **17,** 2148–2155
41. Tamai, K., Semenov, M., Kato, Y., Spokony, R., Liu, C., Katsuyama, Y., Hess, F., Saint-Jeannet, J. P., and He, X. (2000) *Nature* **407,** 530–535
42. Lazar, C. S., Cresson, C. M., Lauffenburger, D. A., and Gill, G. N. (2004) *Mol. Biol. Cell* **15,** 5470–5480
43. Wojcikiewicz, R. J. H. (2004) *Trends Pharmacol. Sci.* **25,** 35–41
44. Heydorn, A., Sondergaard, B. P., Ersboll, B., Holst, B., Nielsen, F. C., Haft, C. R., Whistler, J., and Schwartz, T. W. (2004) *J. Biol. Chem.* **279,** 54291–54303

Adrenomedullin
A Protective Factor for Blood Vessels

Johji Kato, Toshihiro Tsuruda, Toshihiro Kita, Kazuo Kitamura, Tanenao Eto

Abstract—Adrenomedullin (AM) is a vasodilator peptide having a wide range of biological actions such as reduction of oxidative stress and inhibition of endothelial cell apoptosis. The AM gene is expressed in vascular walls, and AM was found to be secreted from cultured vascular endothelial cells, smooth muscle cells, and adventitial fibroblasts. Plasma AM levels in patients with arteriosclerotic vascular diseases are elevated in possible association with the severity of the disease. When administered over a relatively short period, AM dilates blood vessels via an endothelium-dependent or independent mechanism. Experiments in vitro have shown that AM exerts multiple actions on cultured vascular cells, which are mostly protective or inhibitory against vascular damage and progression of arteriosclerosis. Either prolonged infusion or overexpression of AM suppressed intimal thickening, fatty streak formation, and perivascular hyperplasia in rodent models for vascular remodeling or atherosclerosis. Intimal thickening induced by periarterial cuff was more severe in AM gene-knockout mice than their littermates, suggesting a protective role for endogenous AM. Moreover, AM has recently been suggested to possess angiogenetic properties. Collectively, a body of evidence suggests that AM participates in the mechanism against progression of vascular damage and remodeling, thereby alleviating the ischemia of tissues and organs. (*Arterioscler Thromb Vasc Biol.* 2005;25:2480-2487.)

Key Words: adrenomedullin ■ vasodilatation ■ endothelium ■ smooth muscle cell ■ arteriosclerosis

Cardiovascular diseases secondary to arteriosclerosis of blood vessels are currently among the leading causes of death in developed countries. A number of factors, both humoral and mechanical, have been shown to modulate vascular function in humans as well as in experimental animals.[1] Blood vessel dysfunction resulting from an imbalance of those factors accelerates the process of vascular remodeling and atherosclerosis.[1] Vasoconstrictors including angiotensin II and endothelins not always but mostly act as proatherogenic factors, whereas vasodilators, either peptides or non-peptides, such as natriuretic peptides, nitric oxide (NO), and prostaglandin (PG) I_2, have antiatherogenic properties.[1] In 1993, a new vasodilator peptide, adrenomedullin (AM), was isolated from the tissue extract of a human pheochromocytoma by monitoring cAMP levels in rat platelets.[2] Substantial levels of the AM peptide and gene expression were detected in the cardiovascular tissues including blood vessels. As listed in the Table, AM was found to exert a wide range of biological actions related to vascular functions in cultured cells, with which observations in vivo have been mostly accordant. Ever since the discovery of AM, efforts have been made to clarify the role of this bioactive peptide in blood vessels and a substantial amount of basic and clinical data has been accumulated. In this review, after summarizing the biochemical and pharmacological features of AM, we discuss its role in blood vessels, which is assumed to be protective, or inhibitory against the progression of vascular damage and remodeling.

Biochemistry of AM

Human AM is a 52-aa peptide with a ring structure formed by a disulfide bond and amidated tyrosine at the C terminus (Figure 1), both essential for binding to receptors and biological activity.[2–4] Based on sequence homology, AM is thought to belong to the calcitonin gene–related peptide (CGRP) superfamily.[2–4] Cloning of the cDNA encoding AM revealed the AM precursor peptide preproAM to comprise 185 amino acids, with the C terminus followed by a pair of basic amino acids, Arg-Arg, a typical processing signal (Figure 2).[5] In addition to AM, preproAM was found to contain another bioactive peptide, proadrenomedullin N-terminal 20 peptide (PAMP), in the N-terminal portion.[5] PAMP lowered blood pressure when injected intravenously, but its action is weaker than that of AM and there is currently little information available as to the role of PAMP in the vasculature.[3,4] In a sequence analysis of the genomic DNA for human preproAM, AM was found to be encoded in the fourth exon and PAMP in the second and third exons (Figure 2).[6] When processed from preproAM, AM-Gly, an intermediate form (iAM), is produced, and then iAM is converted by the amidation enzyme to the mature form of AM (mAM) having an amide structure at the C terminus.[7] The mature form of PAMP is thought to be produced by a similar process (Figure 2).

Original received May 17, 2005; final version accepted July 11, 2005.
From the First Department of Internal Medicine, Miyazaki Medical College, University of Miyazaki, Japan
Correspondence to Johji Kato, MD, PhD, First Department of Internal Medicine, Miyazaki Medical College, University of Miyazaki, 5200 Kihara, Kiyotake, Miyazaki 889-1692, Japan. E-mail jkjpn@med.miyazaki-u.ac.jp

Arterioscler Thromb Vasc Biol. is available at http://www.atvbaha.org DOI: 10.1161/01.ATV.0000184759.91369.f8

Biological Actions of AM on Cultured Vascular Cells

Cell Type	Observed Effects	Reference No.
Endothelial cells	Elevation of cAMP level	30, 32, 65
	Intracellular Ca^{2+} mobilization	65
	Stimulation of NO production	65
	Stimulation of proliferation and migration	67
	Inhibition of apoptosis	61, 62, 66
Smooth muscle cells	Elevation of cAMP level	21, 34
	Inhibition or stimulation of proliferation	68, 69
	Inhibition of migration	34, 70
	Reduction of oxidative stress	71
Adventitial fibroblasts	Elevation of cAMP level	72
	Inhibition of proliferation	39
	Augmentation of metalloproteinase-2 action	72

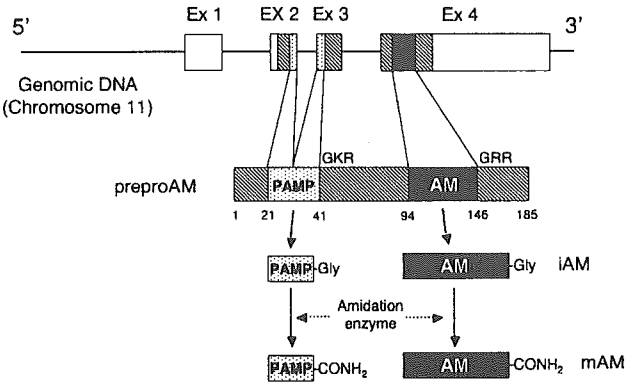

Figure 2. Schematic representations of the AM gene and of the processing of AM and PAMP from preproAM. Ex indicates exon; PAMP, proadrenomedullin N-terminal 20 peptide; iAM and iPAMP, intermediate forms of AM and PAMP, respectively; mAM and mPAMP, mature forms of AM and PAMP, respectively.

In an effort to isolate unknown bioactive peptides having sequence homology with AM, another member belonging to the CGRP superfamily was recently discovered independently by two groups and named intermedin/AM-2.[8,9] Human intermedin/AM-2 consists of 47 amino acid residues with an intramolecular ring structure formed by a disulfide bond and amidated tyrosine at the C terminus, showing structural homology with AM.[8,9] Intermedin/AM-2 was shown to shear the receptors with AM by cultured cells,[8] and in accord with this, it exerted vasodilator actions similar to AM ex vivo.[10] However, data on the biochemical and pharmacological features of this novel peptide are currently very limited, and further characterization, such as the tissue distribution and effects on vascular cells, is necessary to discuss its role in blood vessels.

Vasodilator Action of AM

The biological feature of AM initially characterized was a potent, long-lasting, blood pressure–lowering effect with reduced peripheral resistance after intravenous bolus injection or infusion in a relatively short period of time.[2,11,12] The hypotensive effect of AM observed in those studies was shown to be largely secondary to direct vasodilatation,[11,12] which was further demonstrated by ex vivo studies with isolated rat aorta and with perfused rat mesenteric artery.[13,14]

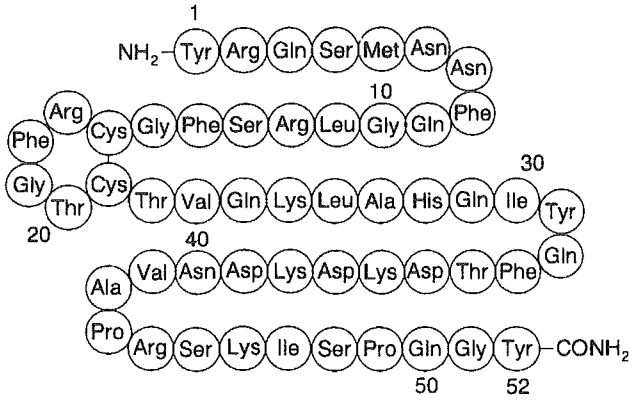

Figure 1. Amino-acid sequence of human AM.

The mechanisms by which AM dilates blood vessels are not completely understood; however, based on the numerous articles published to date, it is clear that AM directly dilates blood vessels of the systemic and pulmonary circulation in an endothelium-dependent or independent manner.[14–23]

AM has been shown to exert an endothelium-dependent vasodilatation via the NO-cyclic GMP (cGMP) pathway in rat aorta, in renal or hindquarter vascular bed of rats, and in canine kidneys.[14–17] In a further analysis of the mechanism, AM dilated rat aorta by activating phosphatidylinositol 3-kinase (PI3K) and Akt via the Ca^{2+}/calmodulin-dependent pathway, which leads to increased production of NO through phosphorylation of endothelial NO synthase.[18] On the other hand, endothelium-independent vasodilatation by AM has also been shown ex vivo in experiments with dog arteries or porcine coronary artery.[19,20] The mechanisms so far proposed for endothelium-independent vasodilatation are an increase in the intracellular cyclic AMP (cAMP) level, a decrease in the Ca^{2+} concentration, and the activation of K^+ channels in vascular smooth muscle cells (SMCs).[21–23]

In humans, similarly to animals, intravenous infusion of AM lowered systemic and pulmonary vascular resistance, reducing blood pressure and increasing heart rate.[24] AM-induced forearm arterial vasodilatation in healthy human subjects was attenuated by N-monomethyl-L-arginine (L-NMMA).[25] In human coronary arterioles, vasodilatation induced by AM ex vivo was found to be dependent on the generation of NO and the activation of K^+ channels, but not on guanylate or adenylate cyclase.[26] A difference between species was also observed regarding the mechanisms. For example, pulmonary vasodilator responses were reduced by N-nitro-L-arginine methyl ester (L-NAME) in rats, but not in cats.[27] Currently, there is little data available on the vasodilator effect on veins, whereas Barder et al reported that vasodilatation of femoral veins in canines was endothelium-dependent, but independent of cAMP and cGMP.[28] Thus, the mechanism by which AM achieves direct vasodilatation appears to differ depending on species, the size of blood vessels, or regions where the vessels are isolated.

Receptors Mediating Vascular Actions of AM

AM has been shown to elevate intracellular cAMP levels in not all but many cells and tissues, including blood vessels, where it exerts biological actions, though identification of the AM receptor subtype has been controversial.[3,4] McLatchie et al identified 3 subtypes of receptor activity–modifying protein (RAMP1 to 3), an accessory protein required for the transport of calcitonin-receptor–like receptor (CRLR) to the cell membrane.[29] CRLR can function as either an AM receptor or a CGRP receptor, depending on the subtype of RAMP expressed: CRLR serves as a CGRP receptor when coexpressed with RAMP1, whereas it functions as an AM receptor when coexpressed with either RAMP2 or 3.[29] AM stimulates intracellular cAMP production in cultured vascular endothelial cells and SMCs,[21,30] and indeed, the mRNAs for CRLR and RAMPs have been detected in these cells and in rat aorta.[31,32] Meanwhile, not all the vascular actions of AM can be fully explained by this receptor system linked to adenylate cyclase: some have been shown to be independent of cAMP.[33,34] This raises the possibility of the presence of unknown receptor systems, and further studies are required to clarify the intracellular signaling for AM.

AM Production in Blood Vessels and Atherosclerotic Lesions

AM was initially isolated from pheochromocytoma tissue, but subsequently the AM gene was found to be expressed in various organs and tissues, including the cardiovascular tissues and cells in humans as well as in rats.[3–5,35] Immunohistochemical studies revealed that three layers of the vessel wall were positive for AM peptide,[35,36] and consistent with this, AM was found to be produced and secreted from 3 types of cultured vascular cells: endothelial cells, SMCs, and adventitial fibroblasts.[37–39] According to Marutsuka et al, AM peptide was expressed in the endothelium of rat aortic arch in a site-dependent fashion, ie, intense immunohistochemical staining for AM was observed in the area where branches begin and on the inner side of the curvature.[40] In these areas, shear stress is relatively low, and indeed, production of AM has been found to be modulated by shear stress in cultured vascular endothelial cells.[41,42] Other factors shown to stimulate production of AM in endothelial cells are oxidative stress and hypoxia.[43,44]

Immunoreactivity for AM was reported to be detected in SMCs of the intima and media of human atherosclerotic lesions.[40] Interestingly, its expression in coronary artery plaques obtained by directional atherectomy was augmented in patients with unstable angina in comparison with stable angina.[45] This finding is consistent with cell culture studies showing that AM production and secretion from cultured vascular SMCs were increased by factors, presumably proatherogenic, such as angiotensin II, endothelin-1, aldosterone, interleukin-1β (IL-1β), and tumor necrosis factor-α (TNF-α).[38,46,47] In addition, aldosterone was shown to stimulate AM production in cultured adventitial fibroblasts as well as in vascular SMCs.[38,39] Macrophages play a pivotal role in the progression of atherosclerotic vascular lesions.[1] Production of AM was detected in macrophages not only in a cell culture experiment,[48] but also by immunohistochemical analysis where intense positive staining was found in advanced atherosclerotic vascular lesion of humans.[40]

Circulating AM in the Bloodstream

Radioimmunoassays for AM revealed that AM peptide was circulating in the blood at mean plasma levels ranging from 2.8 to 10 fmol/mL in healthy human subjects.[7,49,50] Immunoreactive AM in plasma or tissues was found to consist of 2 molecular forms, mAM and iAM (Figure 2), with the major molecular type in plasma and tissues being iAM and mAM, respectively.[7,49–51] As described in the next section, plasma levels of immunoreactive AM were found to be higher in patients with arteriosclerotic vascular diseases than controls, although there was no notable difference in the ratio of mAM and iAM.[52] iAM is thought to have no biological effects by itself, but our ex vivo study showed that iAM dilated rat aorta after its conversion to mAM probably in the aortic wall.[53] Meanwhile, very little information is currently available as to the role of iAM, which should be clarified further with experiments in vivo.

To identify the organs or tissues contributing to the plasma AM level, we examined the plasma levels of AM of various sites in blood vessels of patients with ischemic heart disease.[54] What we found was a step-up in plasma AM levels between the femoral artery and vein.[54] Taking the active secretion of AM from cultured vascular cells into account, it seems likely that the vasculature contributes to the plasma AM level, secreting AM into the bloodstream. On the other hand, there was found to be a step-down between the plasma AM levels of the pulmonary artery and capillary.[54] Substantial levels of AM gene expression were detected in the lungs and the presence of AM peptide in the pulmonary vasculature was immunohistochemically proven,[3–5,55] but the lungs appear to be a target organ or a site for the clearance of circulating AM peptide rather than an AM-secreting organ. Consistent with this notion is the report of abundant expression of AM receptors in the lungs.[56]

Plasma Level of AM in Arteriosclerosis

As an approach to clarifying the role of AM in arteriosclerosis, AM levels in plasma of patients with various types or degrees of arteriosclerotic vascular disease were measured, and the relationships between the plasma levels and the other clinical parameters were examined.[52,57,58] In patients with cerebrovascular disease, a possible association was found between plasma AM levels and endothelial damage by comparing the plasma levels of AM with those of endothelin and thrombomodulin, markers of endothelial damage.[57] Similarly in patients with chronic ischemic stroke, increased plasma AM levels were shown to be associated with the degree of carotid atherosclerosis.[58] Recently, Suzuki et al reported that plasma AM concentrations were elevated in patients with peripheral arterial occlusive disease in proportion to its severity.[52] Moreover, they found close associations between the plasma levels of AM and those of such inflammatory parameters as C-reactive protein and IL-6 in the patients.[52] This finding is not only comparable with the increased production of AM in cultured SMCs by inflammatory cytokines,[46] but also of interest in view of the involve-

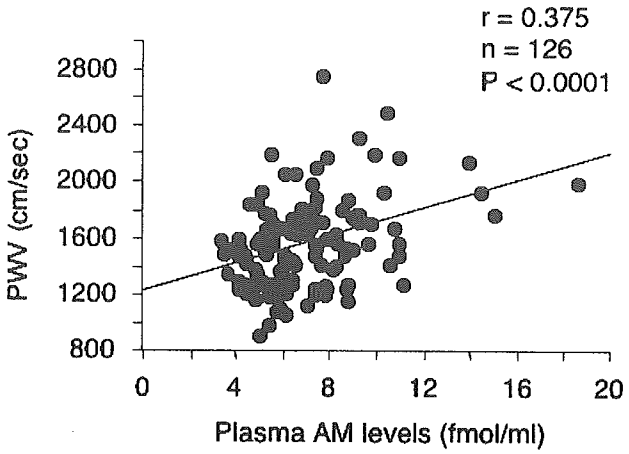

Figure 3. Relationship between the pulse wave velocity (PWV) and plasma AM levels in patients with various degrees of arteriosclerosis. Reprinted from Kita et al [60] with permission from the Japanese Society of Hypertension.

ment of low-grade inflammation in the development and progression of atherosclerotic vascular lesions.[59] Because arterial stiffness is an important cardiovascular risk factor, we measured plasma AM levels in patients with various degrees of atherosclerosis and compared the plasma levels with indirectly measured pulse wave velocity, a parameter used to assess arterial stiffness and sclerosis.[60] As shown in Figure 3, a significant correlation was noted between the plasma AM levels and pulse wave velocity and this relationship was confirmed by multiple regression analysis to be independent of age and blood pressure.[60] These findings are indirect, but indicative of a possible pathophysiological role of AM in arteriosclerotic vascular diseases.

In the latter part of this review, vascular protective effects of AM will be discussed based on the results of cell culture and animal experiments. An important issue we need to mention in this section, therefore, is the significance of the increased plasma AM levels in patients with arteriosclerosis. Because of active production of AM in cultured vascular cells and vessel walls, AM has been assumed to act in a autocrine or paracrine fashion.[3,4,37-40] Indeed, blockade of the actions of endogenous AM with anti-AM antibody or the AM antagonists impaired the vascular protective effects in vitro.[61,62] Meanwhile, according to our experiments in vivo,[63,64] the long-term infusion of AM significantly suppressed neointimal formation and adventitial hyperplasia, raising plasma AM levels by 1 to 2 fmol/mL, an increase within the physiological range. This suggests a possible role for AM, not only as a local modulator, but also as a factor circulating in the blood.

Vascular Protective Effects In Vitro

As discussed in the section Vascular Actions of AM, AM exerts endothelium-dependent vasodilatation, which can be blocked by inhibitors for NO synthase. Consistent with this, in cultured vascular endothelial cells, AM was found to stimulate phospholipase C activation and inositol 1,4,5-triphosphate formation, resulting in an elevation of the intracellular Ca^{2+} level and activation of NO synthase.[65] Kato et al reported that AM inhibited serum deprivation–induced apoptosis of cultured rat vascular endothelial cells.[61] Blockade of the endogenous AM by anti-AM anti-serum impaired the inhibitory effect of the nonimmune serum on apoptosis, suggesting an autocrine or paracrine role for AM.[61] According to the subsequent study by that group, AM upregulated the expression of Max protein, leading endothelial cells to survive.[62] Meanwhile, other adenylate cyclase activators such as PG I_2 and forskolin failed to exert an antiapoptotic effect and a cAMP antagonist was unable to block the effect of AM, therefore a cAMP-independent mechanism seems involved in this action.[61] An antiapoptotic effect of AM was further observed by an independent group. Sata et al found that AM inhibited serum deprivation–induced apoptosis of cultured human umbilical vein endothelial cells.[66] In their experiment, the effect of AM was abrogated by L-NAME, but not by an inhibitor for soluble guanylate cyclase, suggesting an NO-dependent but cGMP-independent mechanism.[66]

Furthermore, AM was shown to cause vascular regeneration by promoting the proliferation and migration of cultured vascular endothelial cells.[67] AM promoted re-endothelialization of wounded human umbilical vein endothelial cells, and this effect was attenuated by inhibitors for protein kinase A and PI3K, suggesting an action mediated by cAMP and the PI3K–Akt pathway.[67] Stimulation of the proliferation and migration of endothelial cells may be involved in the angiogenic action of AM, which will be discussed later in this review. Although the mechanisms of action are still under investigation, these effects of AM on endothelial cells may be protective against vascular damage and arteriosclerosis.

The proliferation of vascular SMCs in the media and intima of arteries is involved in the progression of vascular remodeling or atherosclerotic lesions. Because AM is produced by SMCs in the media, its effects on the proliferation and migration of this type of cell were tested in vitro; however, there has been some inconsistency regarding the actions of AM. AM was shown to inhibit the proliferation of cultured SMCs via a mechanism mediated by cAMP,[68] whereas Iwasaki et al found that AM stimulated proliferation of the cells in a mitogen-activated protein kinase–dependent manner.[69] Horio et al reported an inhibitory effect of AM on the migration of cultured SMCs, which is presumably mediated by intracellular cAMP.[70] Inhibition of the migration of SMCs by AM was confirmed by an independent group,[34] but according to this report, AM inhibited migration via a cAMP-independent mechanism.[34] These discrepancies may have resulted from differences in the experimental conditions or types of cultured cells used, though there has currently been no clear explanation. Meanwhile, as discussed in the next section, recent studies in vivo suggest that AM inhibits intimal hyperplasia induced by periarterial cuff or by intimal balloon injury.

Another vascular protective action of AM recently reported in SMCs was a reduction in the generation of reactive oxygen species (ROS), a group of molecules involved in vascular damage and the progression of arteriosclerosis. The generation of intracellular ROS induced by angiotensin II was inhibited by AM, in a cAMP- and protein kinase A–dependent manner, in cultured vascular SMCs of rats.[71] Moreover,

AM weakened redox-sensitive cellular responses such as the activation of c-Jun amino-terminal kinase (JNK) and gene expression for plasminogen activator inhibitor (PAI)-1, monocyte chemoattractant protein-1, and Nox-1, a component of reduced nicotinamide adenine dinucleotide phosphate (NADPH) oxidase.[71]

Not only the intima and media but also the adventitial layer has been recognized to have a significant role in the process of vascular remodeling. Blood vessels would increase their stiffness if an excessive accumulation of extracellular matrix or proliferation of adventitial fibroblast were to occur. The proliferation of adventitial fibroblasts induced by aldosterone, a factor involved in the fibrosis of cardiovascular tissue, was found to be suppressed by AM, with a concomitant reduction in the activity of extracellular signal-related kinase.[39] Additionally in that study, autocrine or paracrine inhibition by AM was proposed, based on the production of AM by the adventitial fibroblasts and on augmented proliferation by the AM receptor antagonists.[39] By synthesizing and degrading matrix proteins, adventitial fibroblasts are known to modulate the formation of the extracellular matrix in the adventitia. Our recent experiments showed that AM upregulated the enzymatic activity and protein expression of matrix metalloproteinase-2 (MMP-2), which degrades collagens and elastin, in cultured adventitial fibroblasts of rat aorta possibly via the cAMP–protein kinase A pathway.[72] Collectively, these findings suggest a role for AM in modulating adventitial proliferation and extracellular matrix formation.

Vascular Protective Effects In Vivo

As discussed above, plasma AM levels are elevated in patients with various arteriosclerotic vascular diseases, and the findings from cell culture studies have implied a role for AM, which is presumably protective of blood vessels. To investigate whether or not AM has protective effects on vascular damage and remodeling in vivo, 3 experimental approaches have so far been taken: long-term administration of AM, virally-mediated overexpression of AM, and genetic manipulation of the AM gene.

Using the first method, we found that prolonged AM infusion for 2 weeks partially inhibited neointimal hyperplasia induced by balloon injury in rat carotid arteries (Figure 4).[63] Meanwhile, somewhat conflicting findings were obtained by Shimizu et al, who showed that chronic infusion of the AM antagonist CGRP(8–37) inhibited neointimal hyperplasia induced by ballooning in rats.[73] CGRP(8–37) is a CGRP receptor antagonist, which has been able to block some, but not all, the actions of AM in relatively short-term experiments.[16,20,30,62] However, it has yet to be clarified whether or not this antagonist can block the action of endogenous AM when infused chronically. It should be noted that in our study mentioned above, the prolonged infusion of AM suppressed not only balloon injury–induced intimal hyperplasia but also the proliferation of fibroblasts and collagen deposition of the adventitia (Figure 4),[63] a finding consistent with the in vitro inhibitory effect of AM on the proliferation of cultured adventitial fibroblasts.[39] Inhibition of adventitial hyperplasia by AM was confirmed by our study in vivo, in which perivascular fibrosis of coronary arteries of

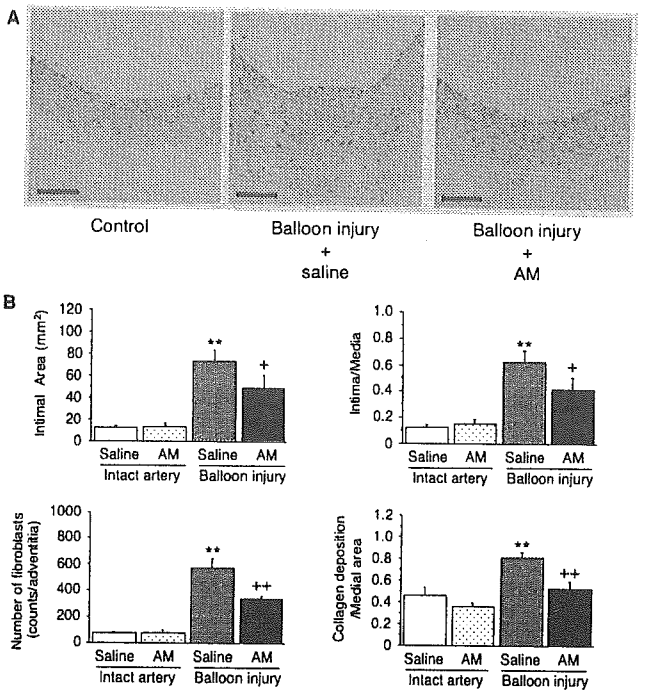

Figure 4. Effects of AM on neointimal and perivascular hyperplasia in rat carotid arteries injured by ballooning. A, Histological findings of the intact and injured arteries of rats infused intravenously with 200 ng/h of AM or saline for 2 weeks. B, Quantitative analyses of intimal and adventitial hyperplasia. Values are the means±SEM; $^{**}P<0.01$ vs intact artery with saline infusion; $^{+}P<0.05$, $^{++}P<0.01$, vs injured artery with saline infusion; bar, 100 μm. Reprinted from Tsuruda et al[63] with permission from Elsevier.

rats infused chronically with angiotensin II was suppressed by coinfusion of AM.[64] This effect was accompanied by the suppression of fibroblast activation and transforming growth factor (TGF)-β1 expression, but not by a significant reduction of blood pressure.[64]

In accord with the effect of prolonged infusion of AM, adenovirus-mediated local delivery of the AM gene was shown to inhibit neointimal hyperplasia of carotid arteries after balloon injury in rats.[74] Interestingly in that study, endothelial regeneration was more pronounced in rats given the AM gene than in the controls,[74] a result consistent with the cell culture experiments, where AM promoted reendothelialization of a wounded monolayer of endothelial cells.[67] The inhibition of neointimal hyperplasia by the AM gene delivery was accompanied by an elevation of tissue cGMP levels, suggesting a mechanism involving the NO–cGMP pathway.[74]

Thirdly, vascular protective effects have been suggested by genetic manipulation of the AM gene in mice. Transgenic mice overexpressing the AM gene (AM-Tg) were found to be resistant to neointimal hyperplasia induced by a periarterial cuff placed on the femoral artery.[75] This resistance seems also to be mediated by the NO–cGMP pathway because it disappeared on administration of L-NAME.[75] Moreover, a protective effect of AM was demonstrated by cross-mating apoE knockout (apoE-KO) mice with AM-Tg. The apoE-KO mice overexpressing AM showed a less extensive hypercholesterolemia-induced fatty streak formation with a greater